System

MECHANICAL

TECHNOLOGY

INCORPORATED

FACILITY FORM 602

N65-35360 (ACCESSION NUMBER)	(THRU)
53 (PAGES)	1 (CODE)
CR 67345 (NASA CR OR TMX OR AD NUMBER)	15 (CATEGORY)

GPO PRICE $ _____

CSFTI PRICE(S) $ _____

Hard copy (HC) $3.00

Microfiche (MF) .50

ff 653 July 65

Rpt 31259

MECHANICAL TECHNOLOGY INC.
968 Albany - Shaker Rd.
Latham, N. Y.

MTI-63TR44

STATIC AND DYNAMIC STIFFNESS AND DAMPING OF THE SOURCE FED ANNULAR THRUST BEARING

by

J. W. Lund

Contract No. NAS 8-5154

LIBRARY LOAN COPY

TECHNICAL REPORT

No. MTI-63TR44
Date Oct. 1963

STATIC AND DYNAMIC STIFFNESS AND DAMPING OF THE SOURCE FED ANNULAR THRUST BEARING

by

J. W. Lund

Jørgen W. Lund
Author(s)

Jørgen W. Lund
Approved by

Approved by

Prepared under
Contract No. Nas 8-5154

Supported by
NATIONAL AERONAUTICS AND SPACE ADMINISTRATION
HUNTSVILLE, ALA.

Reproduction in Whole or in Part is Permitted
for any PURPOSE of the U. S. Government

MECHANICAL TECHNOLOGY INCORPORATED
LATHAM, N.Y.

MTI-23 (1-63)

TABLF OF CONTENTS

	Page
ABSTRACT	iii
INTRODUCTION	1
DISCUSSION	3
RESULTS	6
a. General Data	6
b. Numerical Example, Comparison with Line Source Solution	10
Table 1	13
ANALYSIS	14
Steady State Pressure	16
Dynamic Pressure	17
Finite Difference Equations	20
Static Stiffness and Damping	22
Stability	22
CONCLUSIONS	23
RECOMMENDATIONS	24
REFERENCES	25
APPENDIX: Description of Computer Program	26
Input	26
Output	31
Program Operation	32
Input Forms	34
EXAMPLE OF COMPUTER OUTPUT	
NOMENCLATURE	43

ABSTRACT

35360

A method is presented for calculating the static and the dynamic stiffness and damping of the orifice restricted, externally pressurized gas thrust bearing. The bearing is an annulus and fed from individual orifices. The orifices are treated approximately as point sources. Assuming the vibratory amplitude to be small compared to the clearance a finite difference procedure is used to solve Reynolds equation for the pressure developed in the film. A computer program has been written and gives the results in dimensionless form as functions of 2 variables (possibly 3 variables), namely flow parameters and a frequency number. The procedure for obtaining actual bearing data from the dimensionless results is described.

One numerical example is given and compared to the earlier obtained, less accurate line source solution. As expected the agreement is perfect for choked orifice flow but the difference rapidly increases with decreasing orifice pressure drop. It is uncertain how much of this difference is due to an actual discrepancy and how much is due to the arbitrarily selected value for the feeder hole diameter. Further calculations are needed to clear up the problem.

Finally, it is shown how the results may be presented in concise, readily used design charts with a minimum number of graphs. It is also indicated how the calculations may be used to determine the threshold of instability.

The report includes instructions for preparing the computer input and input forms.

Author

INTRODUCTION

In evaluating the performance of the externally pressurized bearing the dynamic stiffness and damping play an important role. The term "dynamic" refers to the effect of vibratory frequency on the load carrying capacity of the bearing. Since the gas is compressible the gas film acts as an airspring which stiffens as the frequency increases. Furthermore, the load is not completely in phase with the amplitude so that damping also exists.

It is the purpose of the present report to establish theoretical analysis for the calculation of this stiffness and damping. A previous investigation (Ref.1) analyzed the dynamic performance of the hydrostatic journal and thrust bearing assuming sufficiently many orifices that they may be represented by a line source. In the present report only the annular thrust bearing is studied but the gas feeding is now represented more accurately by point sources. Several methods are available for such an analysis as described later. In the present study a numerical solution by finite difference calculations is chosen. Although this method is only approximate from a purely mathematical point of view (especially the source representation) it is believed to resemble the physical conditions as closely as a more refined analysis.

Briefly, the method is based upon the compressible Reynolds equation interpreted as the continuity equation. At the meshpoint in the finite difference mesh, where the source is located, the external flow is introduced. Since the meshpoint represents a finite area the pressure will have a finite value at the source. This differs from the accurate solution where the pressure is infinite at the source. Furthermore, the non-linear Reynolds equation is linearized by assuming small amplitude and harmonic motion. No approximation is involved by the linearization as long as only linear spring and damping coefficients are desired and not the response due to a finite amplitude.

The report emphasizes the analysis and gives only numerical results for one example which is compared to the line source solution of Ref. 1. This comparison, however, furnishes some insight into the approximations involved in the line source solution and seems to give indications why the line feed solution will not always give reliable answers.

DISCUSSION

Approaching the problem of the dynamic load of the source fed hydrostatic bearing several difficulties arise. There is first the problem of bearing geometry. In this respect the journal bearing presents two additional difficulties not existing in the thrust bearing: a) the film thickness in the journal bearing is not uniform, and b) the point sources in the journal bearing do not have the same flow (source strength), requiring the solution of as many non-linear algebraic equations as there are sources. Hence, in order to bring out the essential features more clearly and to establish the general method of approach, it seems logical to obtain the solution for the thrust bearing before attempting the solution of the journal bearing. This is the purpose of the present report.

The pressure in the gas film is given through Reynolds equation which is a non-linear partial differential equation, see Eq. (1). Assuming harmonic motion and small amplitude, a first order perturbation in the amplitude results in two linear partial equations, one for the static pressure and one for the dynamic pressure component. Each of the equations contains a source feeding term but whereas the source strength for the static pressure appears as an independent parameter the dynamic source strength is a function of the dynamic pressure itself. However, this difficulty is easily circumvented making the dynamic pressure the sum of two contributions, denoted G and H, such that in principle G is the frequency contribution and H is the dynamic source feeding contribution. Hence, the total problem is reduced to solving 3 linear partial differential equations: one for the static pressure P_o, one for G and one for H. Of these equations the one for P_o and the one for H contains a source feeding term.

Several methods are available for solving partial differential equations

It is more crude and in itself not an exact solution unless used to establish a limiting process. The method is a direct finite difference solution of the equations including the flow from the source. Covering the annular sector by a finite difference grid the source flow is introduced only at the grid point where the source is located. Since the grid point represents the neighboring area as given by the grid size (i.e. $\Delta r \cdot \Delta\theta$) the solution depends on the grid size. For this reason the grid size around the source is made different from the overall grid size. Thus it is possible to specify a feeder area which is independent of the number of mesh points. The solution, of course, is then dependent on the feeder area but such that for a sufficiently small feeder area the load is independent of this area. It is seen that from a physical point of view the outlined method may be more realistic than the more accurate mathematical solution. In the actual bearing the external flow enters the bearing over a finite feeder area and not at a point. Whereas the described finite difference method results in a finite pressure downstream from the orifice the point source solution yields an infinite pressure at the source such that the downstream pressure is determined by the pressure value at a specified distance from the source. Hence, the point solution is as dependent on the feeder hole radius as is the finite difference method.

with a point source or in other words, to determine the corresponding Green's function. One such method is given in Ref. 1 employing a product solution and resulting in relatively fast convergent infinite series. The disadvantage of the method is the large amount of algebra with a correspondingly large effort of computer programming and the possibility of numerical errors due to computer round-off in the evaluation of the series. Other methods of solution are based upon knowing the nature of the singularity function. Thus the equation for the static pressure P_o^2 is Laplace's equation where the singularity function is the log-function. Hence, subtracting $C \cdot \log r$ (C = source strength) from P_o^2 results in a non-singular equation with a well-behaved variable but with somewhat complex boundary conditions. This reduced equation is more amenable to a solution than the original equation and both analytical and numerical solutions may be obtained. The difficulty arise when neither the singularity function nor the source strength is known which is the case for the dynamic pressure equation. The problem of determining the source strength is eliminated as described earlier but the singularity function has not been established. Referring to Eq. (15) it is seen that the difficulty arises because the dynamic pressure is a function of the static pressure P_o such that P_o appears in a coefficient to the variable. P_o varies both radially and circumferentially and has a singularity. Had P_o been a constant the solution would have been a Bessel function and the singularity function a Neumann function of a complex variable, i.e. logarithmic. Hence, it would be reasonable to expect that the actual singularity function is also logarithmic but upon substitution into Eq. (15) this is not immediately obvious. It is possible that this holds true in a limiting process but until this process has been worked out the reduced equation offers no advantage over the original equation.

Based upon the preceding considerations an alternate method is developed.

RESULTS

General Data

The results as obtained from the computer program contain 6 parameters:

1. The ratio R_1/R_2, where R_1 is outer, R_2 inner radius
2. The ratio R_c/R_2, where R_c is the radius of the feeder hole circle
3. The number of feeder holes N
4. The ratio d/R_c where d is the diameter of the feeder hole
5. The flow parameter q
6. The frequency number σ

For a given bearing geometry only the 2 last parameters are true variables. The ratio d/R_c may also be a parameter depending on q and σ but its nature has not yet been explored.

To cover the performance range of a given bearing geometry calculations for several values of q and σ are necessary. For the static load and stiffness (σ=0) the results may conveniently be given by graphs as illustrated in principle below:

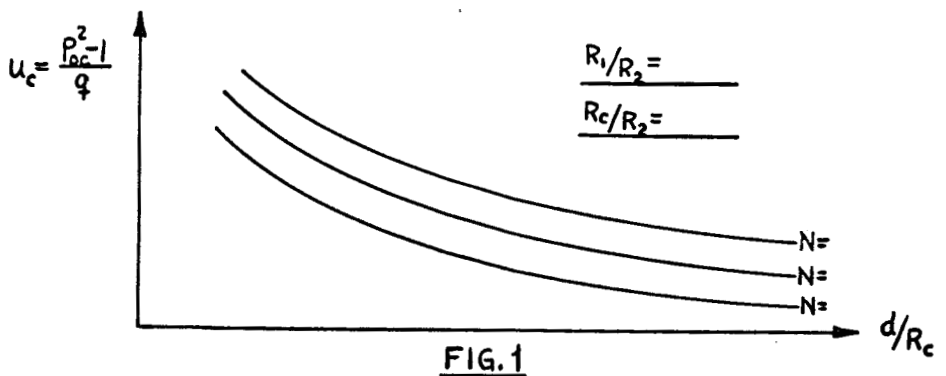

FIG. 1

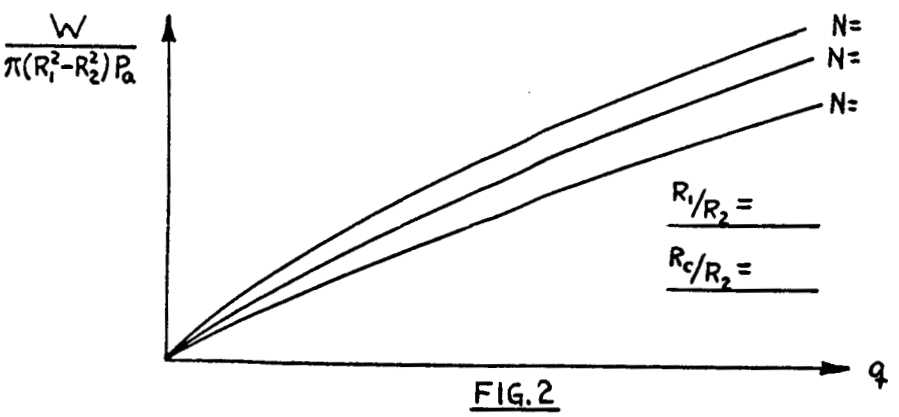

FIG. 2

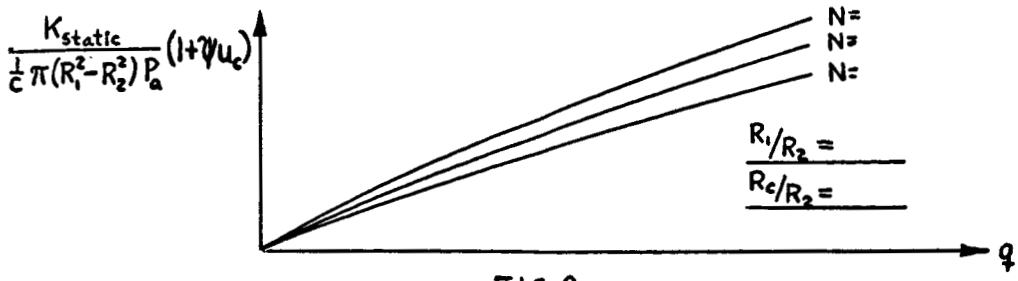

FIG.3

where: P_{oc} = orifice downstream pressure, psia, divided by ambient pressure P_a

$\psi = -\frac{\Lambda_t}{2P_{oc}} \frac{\partial m}{\partial(\frac{P_s}{V})}$ an orifice parameter to be determined as shown below

W = static load, lbs,

K_{static} = static stiffness, lbs/in.

C = film thickness, inch

The procedure for calculating the static load and stiffness shall be outlined:

1. Based on the feeding hole geometry select a feeder hole diameter d and use Figure 1 to determine $U_c = (P_{oc}^2 - 1) / q$.

2. To determine q we have

(1B) $$q = \Lambda_t V m_o$$

where $$\Lambda_t = \frac{6\mu N a^2 \sqrt{\mathcal{R}T}}{P_a C^3}$$

$$V = \frac{P_s}{P_a}$$

μ = viscosity, lbs-sec/in^2

$\mathcal{R}T$ = (gas constant) · (total temperature), in^2/sec^2

a = orifice radius, inch

P_a = ambient pressure, psia

P_s = supply pressure, psia

$$m_o = \frac{M\sqrt{\mathcal{R}T}}{\pi a^2 P_s} = \nu\sqrt{\frac{2k}{k-1}}\left(\frac{P_{oc}}{V}\right)^{1/k}\sqrt{1-\left(\frac{P_{oc}}{V}\right)^{\frac{k-1}{k}}}$$

M = mass flow per orifice lbs-sec/in

ν = vena contracta coefficient

k = ratio of specific heats

Combining the two expressions for q:

(2B) $$\frac{V}{\Lambda_t u_c}\left[\left(\frac{P_{oc}}{V}\right)^2 - \frac{1}{V^2}\right] = m_o$$

where Λ_t and V may be calculated and u_c is determined above. Thus the equation may be solved for the orifice pressure ratio (P_{oc}/V) to get m_o and subsequently q. The solution is best obtained graphically. The right hand side of Eq. (2B) is the orifice flow and a typical curve is given in Fig. 4, where the vena contracta coefficient has been included. The left hand side of Eq.(2B) represents the bearing flow. Since the abcissa in Fig. 4 is $(\frac{P_{oc}}{V})^2$ this flow is represented as a straight line with origin in $\frac{1}{V^2}$ and slope $V/\Lambda_t u_c$. Where the line intersects the orifice curve read off $\frac{P_{oc}}{V}$ and m_o. Use the value of P_{oc}/V to obtain $\frac{\psi V}{\Lambda_t}$ from Fig. 5 where:

$$\frac{\psi V}{\Lambda_t} = -\frac{\partial m}{\partial(\frac{P_c}{V})}\Big/ 2P_c$$

Calculate q from equation (1B) and calculate the orifice parameter ψ.

3. With the found q value read off the dimensionless load from Fig. 2, and multiply by $\pi(R_1^2 - R_2^2)P_a$ to get the load W lbs.

4. With the found q value read off the dimensionless stiffness from Fig. 3 and multiply by $\frac{1}{C}\pi(R_1^2 - R_2^2)P_a \;/\; (1 + \psi u_c)$ to obtain the static stiffness in lbs/in.

5. The mass flow is obtained from:

(3B) $$M_T = \frac{\pi C^3 P_a^2}{6\mu \mathcal{R} T}\cdot q \qquad \text{lbs/sec}$$

(in lbs/sec if $\mathcal{R}T$ is inch)

Turning to the dynamic load it is the sum of two contributions, one stemming from the frequency, denoted A_D, B_D and G_c below and one predominantly

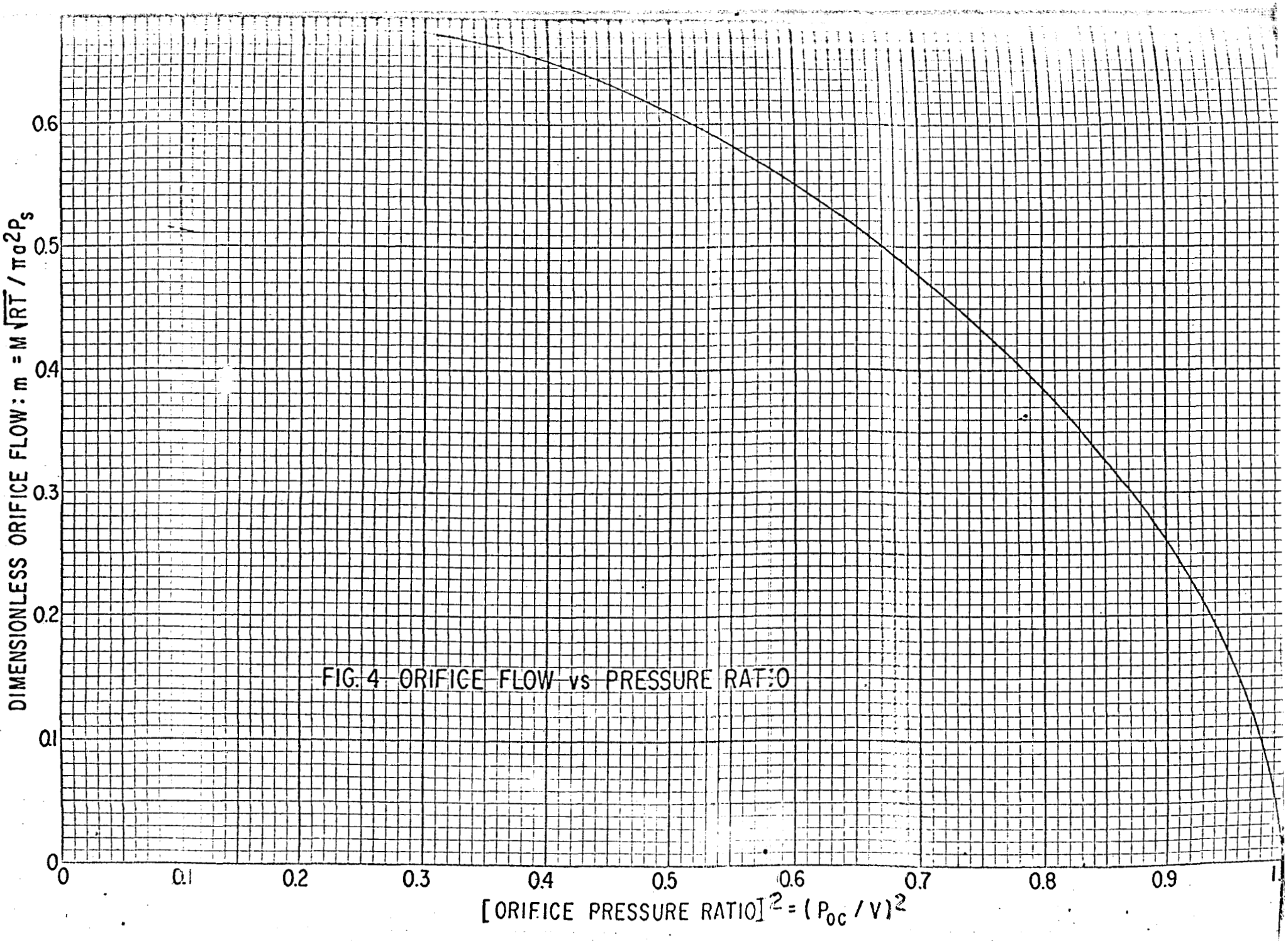

FIG. 4 ORIFICE FLOW vs PRESSURE RATIO

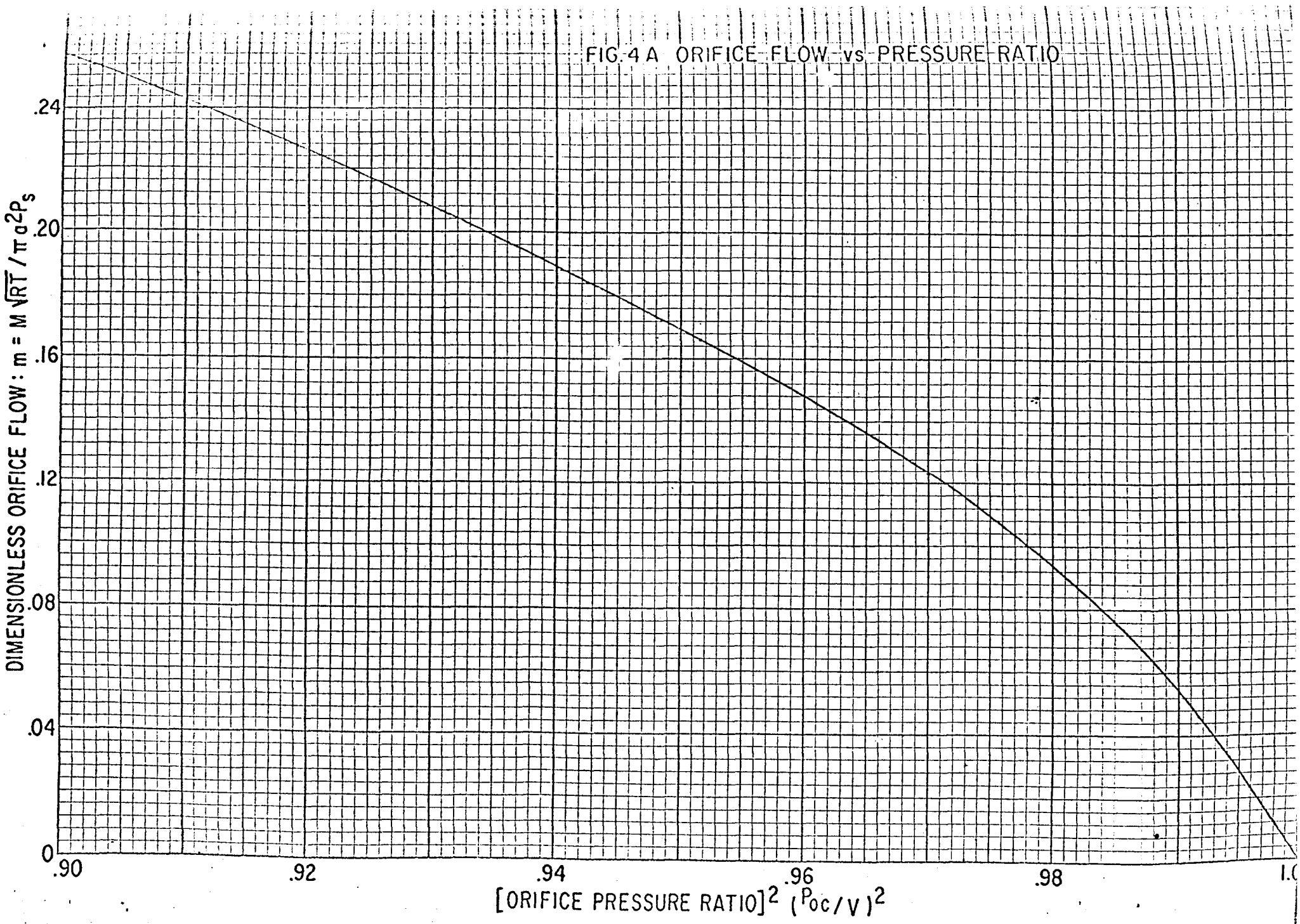
FIG. 4 A ORIFICE FLOW vs PRESSURE RATIO
DIMENSIONLESS ORIFICE FLOW : $m = M\sqrt{RT}/\pi a^2 P_s$
.24
.20
.16
.12
.08
.04
0
.90
.92
.94
.96
.98
1.0
[ORIFICE PRESSURE RATIO]^2 $(P_{oc}/V)^2$

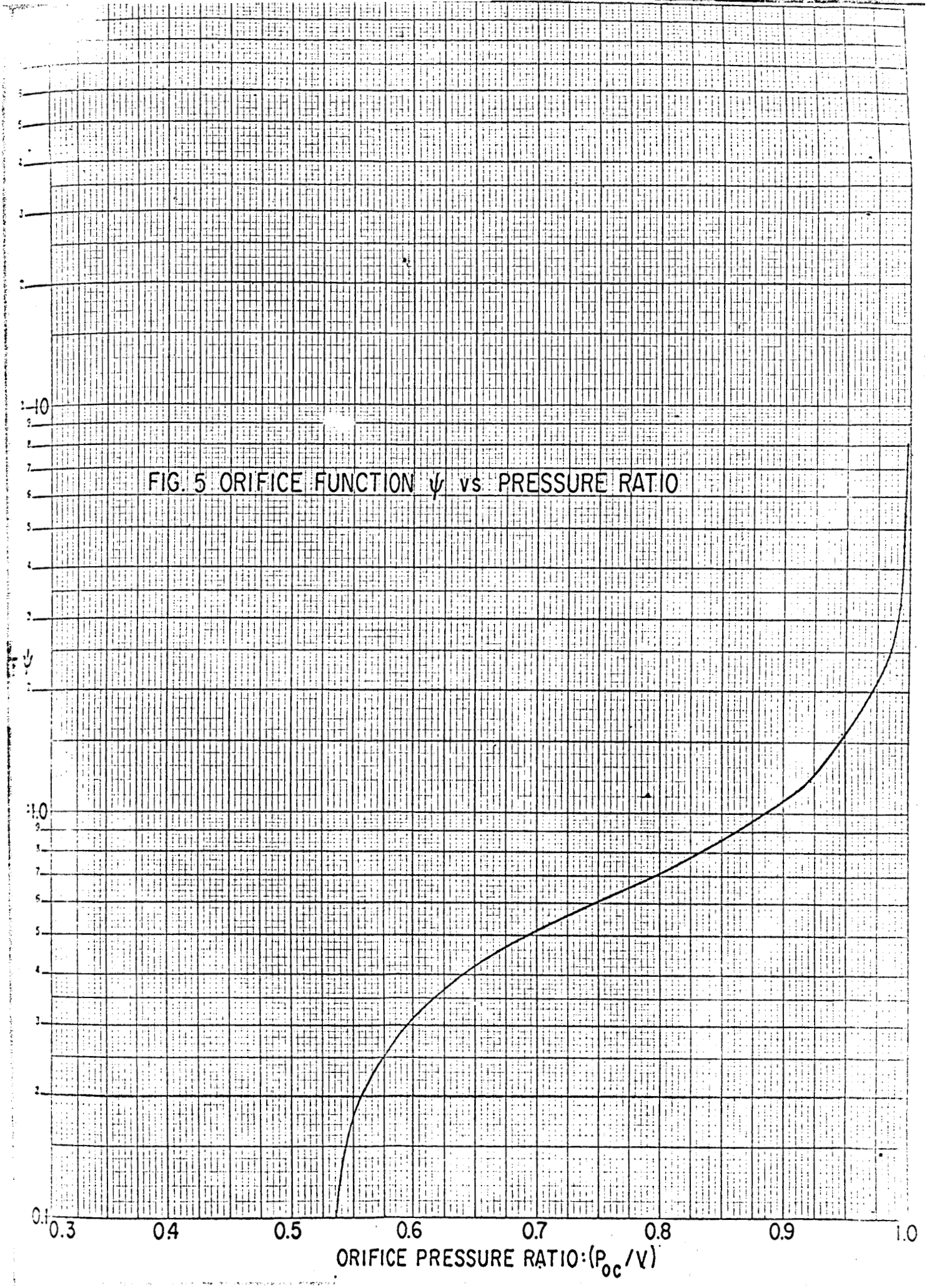

FIG. 5 ORIFICE FUNCTION ψ vs PRESSURE RATIO

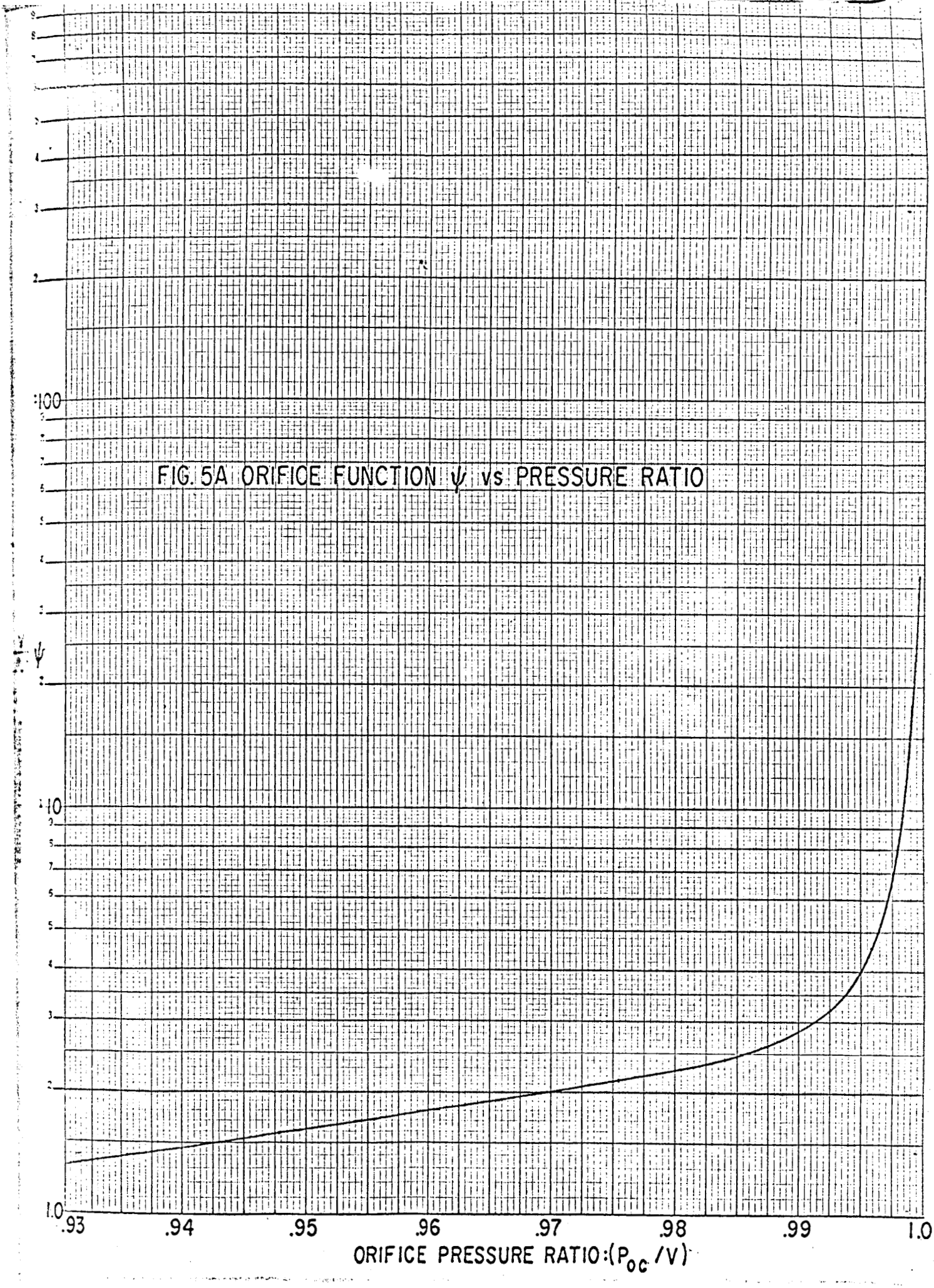

FIG. 5A ORIFICE FUNCTION ψ vs PRESSURE RATIO

from the dynamic source feeding, denoted C_D, D_D and H_c below. The details are given in the analysis but the application of the results shall be described in this section.

The computer calculates the dynamic load contributions A_D, B_D, C_D and D_D and the source parameters G_c and H_c (complex numbers) as functions of the flow parameter q and the frequency number σ:

(4B) $$\sigma = \frac{12\mu\omega}{P_a}\left(\frac{R}{C}\right)^2$$

where: ω = Frequency, rad/sec.

Hence, eight graphs of the general form below are needed:

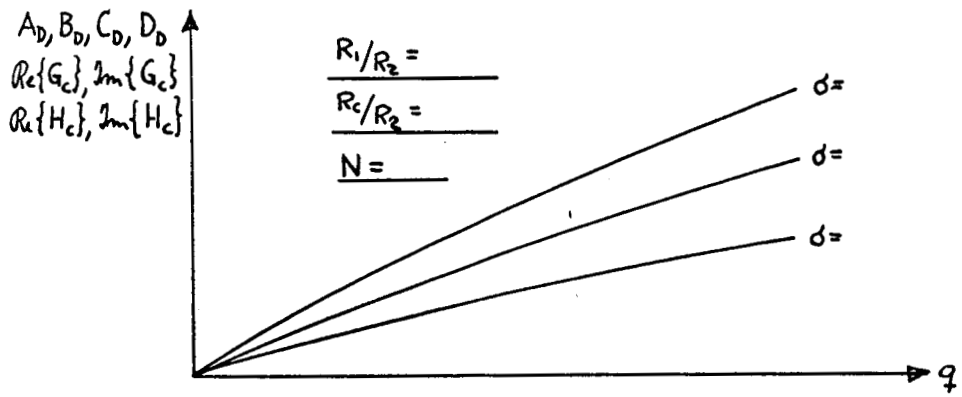

Fig. 6

Having determined q and computed σ the 8 coefficients may be evaluated. Then:

(5B) dimensionless dynamic stiffness = $$\frac{K}{\frac{1}{C}\pi(R_1^2-R_2^2)P_a} = A_D + E_D C_D - F_D D_D$$

(6B) dimensionless damping = $$\frac{\omega B}{\frac{1}{C}\pi(R_1^2-R_2^2)P_a} = B_D + F_D C_D + E_D D_D$$

where E_D and F_D represents the orifice characteristic:

(7B) $$E_D + iF_D = \frac{\frac{3}{2}q - \psi_D G_c}{1+\psi_D H_c}$$

The equation has been left in complex form because Ψ_D may be complex. To illustrate, let the volume in the feeder hole between the orifice and the bearing be V_c in^3. Let it be assumed that the gas pressure in this volume is the previously determined downstream orifice pressure P_{oc} (dimensionless with respect to P_a). Then:

$$\Psi_D = \Psi + i \frac{\sigma}{4P_{oc}} \frac{NV_c}{\pi R_c^2 C} = \Psi + i\Psi_1 \tag{8B}$$

It is seen that $\frac{NV_c}{\pi R_c^2 C}$ expresses the ratio between total feeder hole volume and the volume of the gas film. The larger this ratio becomes, the larger is the phase lag between pressure change and flow change.

b. Numerical Example

A numerical calculation is performed with:

$$\frac{R_1}{R_2} = 1.5$$

$$\frac{R_c}{R_2} = 1.25$$

$$\frac{d}{R_c} = .030$$

$$N = 12$$

$$q = 15$$

$$\sigma = 5$$

The finite difference mesh is 8 × 5. A maximum of 70 iterations are performed, not enough to ensure full convergence but the error is not larger than 4 percent. From the computer output:

$u_c = .6525$

$Re(G_c) = .0029096$ $\quad Im(G_c) = .1122$

$Re(H_c) = .6514$ $\quad Im(H_c) = -.007389$

$P_{oc} = 3.2845$

$$\frac{W}{\pi (R_1^2 - R_2^2) P_a} = .5413$$

For dynamic stiffness: $A_D = .001472$
$C_D = .05708$
$D_D = -.002546$

For damping: $B_D = .1340$
$C_D = .1660$
$D_D = -.007407$

It is desired to compare this solution to the line source solution. This is done for several pressure ratios as listed in Table 1. The calculation procedure is: For given V, compute P_{oc}/V (P_{oc} given from computer). Enter Figs. 4 and 5 to find m_o and $\psi V/\Lambda_t$. Calculate $\Lambda_t = q/Vm_o$ and ψ. Based on ψ-value calculate dynamic stiffness from Eq. (5B) and the damping from Eq. (6B). Note, that in this case the dimensionless damping has the form:

$$\frac{B}{\mu R_1 \cdot \left(\frac{R_1}{c}\right)^2}$$

to make it independent of frequency explicitly.

To illustrate the interpretation of the comparison in Table 1 take V = 3.8 as an example. The first four columns list the values calculated from the point source solution above and let it be assumed for convenience that they accurately represent the actual bearing. The five next columns are the line source solution for the same values of the feeding parameter Λ_t. Thus they give the load, stiffness and flow that would be obtained if the line source solution was used for designing the bearing with the same filmthickness as for the source solution. For V = 3.8 a load of .7866 atm. would be expected whereas the actual bearing at the same clearance can only provide .541 atm. Furthermore, the flow would only be 15/23.52 = .64 of the expected flow. In practice, however, the load is fixed and the desired clearance cannot be maintained. This is the reason for giving the four next columns in Table 1, listing the line source results for the same load as the point source solution ($q_{line} = q_{point\ source}$) and a comparison between the two solutions is carried out in the last three columns. It is seen that the actual

clearance is only .877 of the expected clearance, the actual flow is .675 of the expected value and the stiffness is reduced to .452 of the expected stiffness.

Although this trend qualitatively seems to agree with some of the experimental data obtained by NASA it must be remembered that the given point source calculation is based on an assumed feeding hole diameter. Whereas the load calculation is rather insensitive to changes in feeding hole diameter this is not the case with the orifice downstream pressure P_{oc}. Since all other quantities, except load, are computed on basis of P_{oc} it is necessary to perform several more calculations, evaluating the effect of feeding hole diameter, before valid conclusions can be drawn. Thus the differences in results in Table 1 are largely due to the great discrepancies in orifice pressure ratio.

It may be noted that the point source solution predicts negative damping for pressure ratios of 5.5 and larger, i.e. an unstable bearing. This should not necessarily be taken too seriously in the present case since, as earlier stated, the computer results for A_D and B_D are obtained with a 4 per cent error margin. In calculating the damping this error is rather significant. Still, in principle, the computer program may be used to calculate the threshold of instability, occurring when either the stiffness or the damping turns negative. Combining this procedure with the above given equation for ψ_D the influence of feeder hole volume on the bearing stability may be assessed.

TABLE 1

COMPARISON BETWEEN POINT SOURCE AND LINE SOURCE SOLUTION

Point Source					Line Source, Same Clearance					Line Source, same Load				Same Load		
$V = P_s/P_a$	P_{oc}/V	Λ_t	Dim. Stiff.	Dim. Damp.	P_{oc}/V	Dim. Load	Dim. Stiff.	Dim. Damp.	q	Λ_t	P_{oc}/V	Dim. Stiff.	Dim. Damp.	$\frac{Q_{source}}{Q_{line}}$	$\frac{C_{source}}{C_{line}}$	$\frac{K_{source}}{K_{line}}$
3.4	.966	22.19	.0581	.0946	.840	1.062	.5905	.0097	35.26	7.07	.613	.522	.0079	.319	.683	.163
3.5	.938	14.91	.1031	.0846	.764	.9516	.6069	.0074	30.35	6.76	.594	.509	.0075	.453	.768	.264
3.8	.864	9.076	.1892	.0589	.632	.7866	.5498	.0050	23.52	6.11	.538	.477	.0059	.675	.877	.452
4.0	.821	7.551	.2202	.0451	.575	.7267	.5110	.0042	21.20	5.68	.510	.454	.0052	.752	.909	.534
4.5	.730	5.644	.2512	.0202	.473	.6231	.4196	.0038	17.39	4.99	.451	.386	.0054	.885	.960	.677
5.0	.657	4.678	.2542	.0033	.412	.5838	.3472	.0049	16.02	4.42	.404	.334	.0056	.946	.982	.774
5.5	.597	4.072	.2490	-.010	.369	.5640	.2997	.0054	15.33	4.01	.367	.296	.0056	.986	.995	.843
6.0	.547	3.664	.2443	-.024	.335	.5557	.2663	.0056	15.05					1.0	1.0	.918
8.0	.411	2.738	.1837	-.033	.251	.5541	.1897	.0057	15.0					1.0	1.0	1.0
10.0	.328	2.191	.1429	-.033	.201	.5541	.1476	.0057	15.0					1.0	1.0	1.0

ANALYSIS

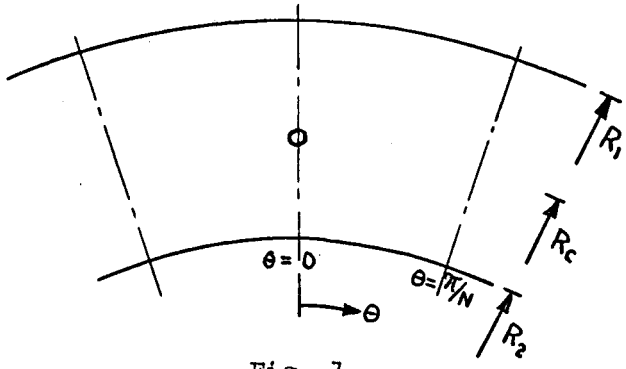

Fig. 7

The thrust bearing is an annulus with inner radius R_2 and outer radius R_1. It is fed through N feeding holes located on the radius R_c. The film thickness is $\bar{h}$. The pressure $\bar{P}$ developed in the film is given through Reynolds equation:

$$(1)\quad \frac{1}{\bar{r}}\frac{\partial}{\partial \bar{r}}\left[\bar{r}\frac{\bar{h}^3}{12\mu}\bar{\rho}\frac{\partial \bar{P}}{\partial \bar{r}}\right] + \frac{\partial}{\bar{r}\partial\theta}\left[\frac{\bar{h}^3}{12\mu}\bar{\rho}\frac{\partial \bar{P}}{\bar{r}\partial\theta}\right] = \frac{\partial(\bar{\rho}\bar{h})}{\partial t} - \frac{M}{R_c\,\delta\theta\,\delta\bar{r}}\Big|_{orifice}$$

where $\bar{\rho}$ is the density and $\frac{M}{R_c\delta\theta\,\delta\bar{r}}$ is the flow per unit area from the feeding holes. To make dimensionless set:

$$(2)\quad r = \frac{\bar{r}}{R_c} \qquad h = \frac{\bar{h}}{C} \qquad P = \frac{\bar{P}}{P_a} \qquad \tau = \omega t$$

and assume isothermal conditions such that $\bar{\rho} = \frac{\bar{P}}{\mathcal{R}T}$ to get:

$$(3)\quad \frac{1}{r}\frac{\partial}{\partial r}\left[r h^3 \frac{\partial P^2}{\partial r}\right] + \frac{\partial}{r\partial\theta}\left[h^3\frac{\partial P^2}{r\partial\theta}\right] = 2\sigma\frac{\partial(Ph)}{\partial\tau} - \Lambda_t V m \frac{4\pi/N}{\delta\theta\,\delta r}$$

where:

$$(4)\quad \sigma = \frac{12\mu\omega}{P_a}\left(\frac{R_c}{C}\right)^2 \qquad \text{Frequency number}$$

$$(5)\quad \Lambda_t = \frac{6\mu N a^2\sqrt{\mathcal{R}T}}{P_a C^3} \qquad \text{Feeding parameter}$$

$$(6)\quad V = \frac{P_s}{P_a} \qquad \text{Pressure ratio}$$

$$(7)\quad m = \frac{M\sqrt{\mathcal{R}T}}{\pi a^2 P_s} \qquad \text{Dimensionless flow}$$

In order to determine the dynamic load let the dimensionless film thickness be:

(8) $$h = 1 - \varepsilon e^{i\tau}$$

such that the motion is harmonic with angular frequency ω and amplitude $\mathcal{R}e(C\varepsilon e^{i\omega t})$. Express the pressure by:

(9) $$P = P_0 + \varepsilon e^{i\tau} P_1$$

Assume $\varepsilon \ll 1$ so that:

(10) $$h^3 = 1 - 3\varepsilon e^{i\tau}$$

(11) $$P^2 = P_0^2 + 2\varepsilon e^{i\tau} P_0 P_1$$

(12) $$m = m_0 + \frac{\varepsilon e^{i\tau}}{V P_{0c}} \frac{\partial m}{\partial(\frac{P_c}{V})}\Big|_{\varepsilon=0} (P_0 P_1)_c = m_0 - 2\varepsilon e^{i\tau} \frac{\psi}{\Lambda_t V} (P_0 P_1)_c$$

where

(13) $$\psi = -\frac{\Lambda_t}{2 P_{0c}} \frac{\partial m}{\partial(\frac{P_c}{V})}\Big|_{\varepsilon=0}$$

and subscript C refers to downstream of the feeding hole. Substitute Eq.(9), (10), (11) and (12) into Eq. (13) to get:

(14) $$\frac{1}{r}\frac{\partial}{\partial r}\left[r \frac{\partial P_0^2}{\partial r}\right] + \frac{\partial^2 P_0^2}{r^2 \partial \theta^2} = -q \frac{4\pi/N}{\delta\theta\,\delta r}$$

(15) $$\frac{1}{r}\frac{\partial}{\partial r}\left[r \frac{\partial (P_0 P_1)}{\partial r}\right] + \frac{\partial^2 (P_0 P_1)}{r^2 \partial \theta^2} - \frac{i\sigma}{P_0}(P_0 P_1) = -i\sigma P_0 - \left[\frac{3}{2} q - \psi (P_0 P_1)_c\right] \frac{4\pi/N}{\delta\theta\,\delta r}$$

where:

(16) $$q = \Lambda_t V m_0$$

Eq. (14) and (15) are to be solved with the boundary conditions:

(17) $$r = \begin{cases} \frac{R_1}{R_c} \\ \frac{R_2}{R_c} \end{cases} : \quad P_0 = 1 \qquad P_1 = 0$$

$$(18) \qquad \Theta = \begin{cases} 0 \\ \frac{\pi}{N} \end{cases} : \quad \frac{\partial P_0}{\partial \theta} = 0 \qquad \frac{\partial P_1}{\partial \theta} = 0$$

Steady State Pressure

The steady state pressure P_o derives from Eq. (14). It is convenient to make the equation homogenous by introducing.

$$(19) \qquad u = \frac{P_o^2 - 1}{q}$$

so that Eq. (14) becomes:

$$(20) \qquad \frac{1}{r}\frac{\partial}{\partial r}\left[r\frac{\partial u}{\partial r}\right] + \frac{\partial^2 u}{r^2 \partial \theta^2} = -\frac{4\pi/N}{\delta\theta\,\delta r}$$

with the boundary conditions;

$$(21) \qquad r = \begin{cases} \frac{R_1}{R_c} \\ \frac{R_2}{R_c} \end{cases} : u = 0 \qquad \theta = \begin{cases} 0 \\ \frac{\pi}{N} \end{cases} : \frac{\partial u}{\partial \theta} = 0$$

The equation is solved by finite difference methods as shown later. In order to determine P_o it is necessary to find q. This is done by equating the orifice flow to the flow through the bearing. The dimensionless orifice flow m_o is a function of the pressure ratio V and the dimensionless downstream pressure P_{oc}:

$$(22) \qquad m_o = \begin{cases} \nu\sqrt{\frac{2k}{k-1}}\left(\frac{P_{oc}}{V}\right)^{1/k}\sqrt{1-\left(\frac{P_{oc}}{V}\right)^{\frac{k-1}{k}}} & \underline{1 \geq \frac{P_{oc}}{V} \geq \left(\frac{2}{k+1}\right)^{\frac{k}{k-1}}} \\ \nu\sqrt{\frac{2k}{k+1}}\left(\frac{2}{k+1}\right)^{\frac{1}{k-1}} & \underline{0 \leq \frac{P_{oc}}{V} \leq \left(\frac{2}{k+1}\right)^{\frac{k}{k-1}}} \end{cases}$$

Hence, from Eq. (19):

$$(23) \qquad \frac{V}{\Lambda_t u_c}\left[\left(\frac{P_{oc}}{V}\right)^2 - \frac{1}{V^2}\right] = m_o$$

which may be solved for $\frac{P_{oc}}{V}$ and m_o and thus determine $q = \Lambda_t V m_o$.
The solution may be obtained graphically as shown below:

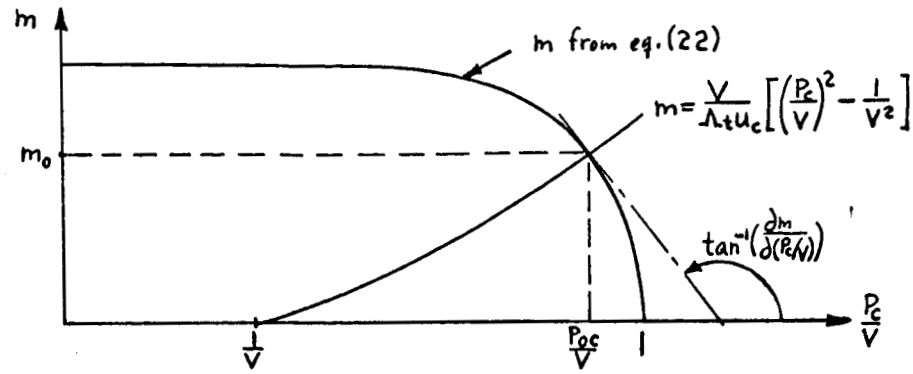

Fig. 8

The dimensionless static load becomes:

$$\frac{W}{\pi(R_1^2-R_2^2)P_a} = \frac{2N/\pi}{(\eta^2 - 1/\gamma^2)} \int_{\frac{1}{\gamma}}^{\eta} \int_0^{\frac{\pi}{N}} \left[\sqrt{1+qu} - 1\right] r\,d\theta\,dr \tag{24}$$

where:

$$\eta = \frac{R_1}{R_c} \tag{25}$$

$$\gamma = \frac{R_c}{R_2} \tag{26}$$

Dynamic Pressure

The dynamic pressure is P_1 as defined by Eq. (9) and given through Eq. (15). To solve Eq. (15) it is convenient to introduce:

$$P_oP_1 = G + \left[\tfrac{3}{2}q - \psi\cdot(P_oP_1)_c\right]H \tag{27}$$

Eq.(27) may be used to express $(P_oP_1)_c$ in terms of G_c and H_c:

$$(P_oP_1)_c = \frac{G_c + \frac{3}{2}qH_c}{1+\psi H_c} \tag{28}$$

So that Eq. (27) may be written:

$$P_oP_1 = G + \frac{\frac{3}{2}q - \psi G_c}{1+\psi H_c} H \tag{29}$$

G and H are determined by:

$$\frac{1}{r}\frac{\partial}{\partial r}\left[r\frac{\partial G}{\partial r}\right]+\frac{\partial^2 G}{r^2\partial\theta^2}-\frac{i\sigma}{P_0}G=-i\sigma P_0 \tag{30}$$

$$\frac{1}{r}\frac{\partial}{\partial r}\left[r\frac{\partial H}{\partial r}\right]+\frac{\partial^2 H}{r^2\partial\theta^2}-\frac{i\sigma}{P_0}H=-\frac{4\pi/N}{\delta\theta\,\delta r} \tag{31}$$

where G and H have the same boundary conditions as P_1 in Eqs.(17) and (18). The equations are solved by finite difference methods as shown later. The dimensionless dynamic load becomes:

$$\frac{W_D/C\varepsilon}{\frac{1}{C}\pi(R_1^2-R_2^2)P_a}=\frac{2N/\pi}{(\eta^2-1/\gamma^2)}e^{i\omega t}\left[\int_{\frac{1}{\gamma}}^{\eta}\int_0^{\frac{\pi}{N}}\frac{G}{P_0}r\,d\theta\,dr+\frac{\frac{3}{2}q-\psi G_c}{1+\psi H_c}\int_{\frac{1}{\gamma}}^{\eta}\int_0^{\frac{\pi}{N}}\frac{H}{P_0}r\,d\theta\,dr\right] \tag{32}$$

where the real part of the right hand side applies. For a better interpretation of Eq. (32) introduce the abbreviations:

$$A_D+iB_D=\frac{2N/\pi}{(\eta^2-1/\gamma^2)}\int_{\frac{1}{\gamma}}^{\eta}\int_0^{\frac{\pi}{N}}\frac{G}{P_0}r\,dr\,d\theta \tag{33}$$

$$C_D+iD_D=\frac{2N/\pi}{(\eta^2-1/\gamma^2)}\int_{\frac{1}{\gamma}}^{\eta}\int_0^{\frac{\pi}{N}}\frac{H}{P_0}r\,d\theta\,dr \tag{34}$$

$$E_D+iF_D=\frac{\frac{3}{2}q-\psi G_c}{1+\psi H_c} \tag{35}$$

so that Eq. (32) may be written:

$$\frac{W_D}{\frac{1}{C}\pi(R_1^2-R_2^2)P_a}=C\varepsilon e^{i\omega t}\left[A_D+E_DC_D-F_DD_D+i\left(B_D+F_DC_D+E_DD_D\right)\right] \tag{36}$$

Since the amplitude is $C\varepsilon e^{i\omega t}$ the velocity is $i\omega C\varepsilon e^{i\omega t}$. Hence, Eq. (36) becomes

$$W_D=K\cdot C\varepsilon e^{i\omega t}+B\,i\omega C\varepsilon e^{i\omega t}$$

where K is the stiffness and B is the damping coefficient, given in dimensionless form by:

$$(37) \qquad \frac{K}{\frac{1}{c}\pi(R_1^2-R_2^2)P_a} = A_D + E_D C_D - F_D D_D$$

$$(38) \qquad \frac{\omega B}{\frac{1}{c}\pi(R_1^2-R_2^2)P_a} = B_D + F_D C_D + E_D D_D$$

In order to make the dimensionless damping coefficient independent of frequency explicitly Eq. (38) can be given the alternate forms:

$$(39) \qquad \frac{B}{\mu R_1 \left(\frac{R_1}{c}\right)^3} = \frac{24N}{\sigma\eta^4}\left[\frac{B_D+F_D C_D+E_D D_D}{\frac{2N/\pi}{(\eta^2-1/\gamma^2)}}\right]$$

$$(40) \qquad \frac{M_0 \mathcal{R} T\, B}{P_a^2 R_1^4} = \frac{4\pi q}{\sigma\eta^4}\left[\frac{B_D+F_D C_D+E_D D_D}{\frac{2N/\pi}{(\eta^2-1/\gamma^2)}}\right]$$

It should be noted that ψ represents the change in orifice flow due to a change in the downstream pressure. Hence, if the feeder hole volume is appreciable, or if there is a recess, there will be a phase lag between flow and pressure change causing ψ to be complex:

$$(41) \qquad \psi = |\psi| e^{-i\varphi}$$

Theoretically $|\psi|$ and φ could be determined by measuring the flow M as a function of Sinusoidal changing downstream pressure P_c:

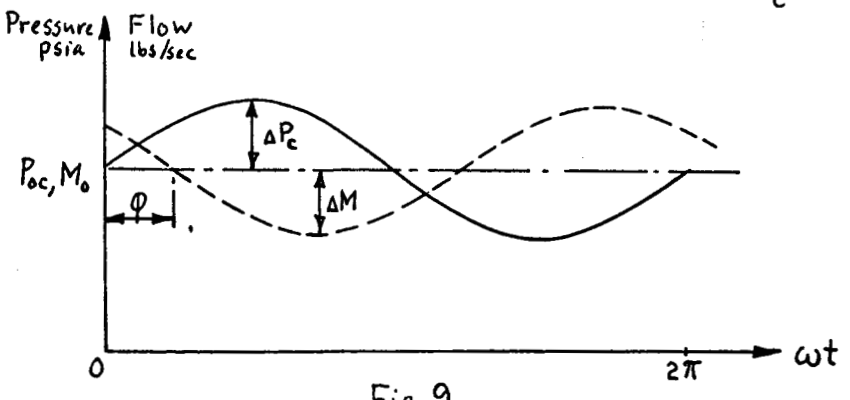

Fig. 9

Then:

$$(42) \qquad |\psi| = \frac{3\mu N \mathcal{R}T}{\pi C^3} \cdot \frac{\Delta M}{P_{oc} \cdot \Delta P_c} = \frac{q}{2} \cdot \frac{P_a^2}{P_{oc} \cdot \Delta P_c} \cdot \frac{\Delta M}{M_o}$$

where $\mathcal{R}T$ is given in inch, P_{oc} and ΔP_c are psia and ΔM is $\frac{\text{lbs}}{\text{sec}}$.

Finite Difference Equations

Eqs(20), (30) and (31) are solved as finite difference equations. The annular sector is subdivided into m radial increments, and n circumferential increments. The feeding hole is ℓ increments from the inner edge. In order to represent the feeding area independently of the overall mesh size additional grid lines are provided around the feeding hole such that the feeding area becomes $\delta^2 = \frac{\pi}{4}$ (feeding hole diameter)^2. This is best shown by a figure:

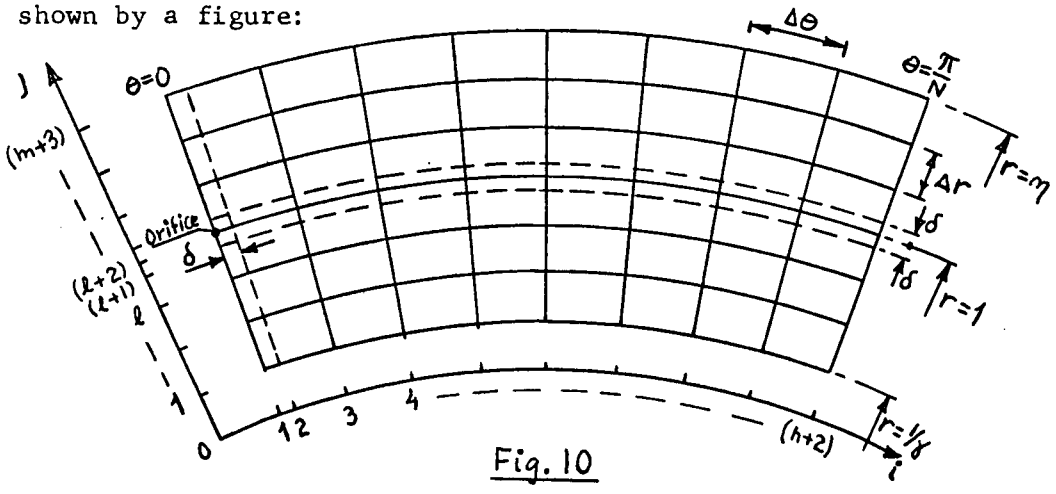

Fig. 10

Let the variables u, G and H be represented by y. Then the general finite difference equation becomes:

$$(43) \qquad y_{ij} = \frac{\left(\frac{r_j}{\Delta r_{j+\frac{1}{2}}} + \frac{1}{2}\right) y_{i,j+1} + \left(\frac{r_j}{\Delta r_{j-\frac{1}{2}}} - \frac{1}{2}\right) y_{i,j-1} + \frac{\left(\frac{\Delta r_{j+\frac{1}{2}}}{r_j} + \frac{\Delta r_{j-\frac{1}{2}}}{r_j}\right)}{\left(\Delta\theta_{i+\frac{1}{2}} + \Delta\theta_{i-\frac{1}{2}}\right)} \left[\frac{y_{i+1,j}}{\Delta\theta_{i+\frac{1}{2}}} + \frac{y_{i-1,j}}{\Delta\theta_{i-\frac{1}{2}}}\right] + i\sigma P_{0,ij} \frac{r_j}{2}\left(\Delta r_{j+\frac{1}{2}} + \Delta r_{j-\frac{1}{2}}\right) + \left.\frac{4\pi/N}{\delta}\right|_{1,\ell+2}}{\frac{r_j}{\Delta r_{j+\frac{1}{2}}} + \frac{r_j}{\Delta r_{j-\frac{1}{2}}} + \frac{\left(\frac{\Delta r_{j+\frac{1}{2}}}{r_j} + \frac{\Delta r_{j-\frac{1}{2}}}{r_j}\right)}{\left(\Delta\theta_{i+\frac{1}{2}} + \Delta\theta_{i-\frac{1}{2}}\right)} \left[\frac{1}{\Delta\theta_{i+\frac{1}{2}}} + \frac{1}{\Delta\theta_{i-\frac{1}{2}}}\right] + \frac{i\sigma}{P_{0,ij}} \frac{r_j}{2}\left(\Delta r_{j+\frac{1}{2}} + \Delta r_{j-\frac{1}{2}}\right)}$$

This equation applies to u, G and H with the modifications:

$$(44)\qquad y = \begin{cases} u & \text{for } \delta = 0 \text{ in eq.(43)} \\ G & \text{for } \left.\dfrac{4\pi/N}{\delta}\right|_{1,\ell+2} = 0 \text{ in eq.(43)} \\ H & \text{for } i\delta P_{0,ij}\,\dfrac{r_j}{2}\left(\Delta r_{j+\frac{1}{2}} + \Delta r_{j-\frac{1}{2}}\right) = 0 \text{ in eq.(43)} \end{cases}$$

The boundary conditions are:

$$(45)\qquad \begin{aligned} y_{i,1} &= 0 \\ y_{i,m+3} &= 0 \\ y_{0,j} &= y_{2,j} \\ y_{n+3,j} &= y_{n+1,j} \end{aligned}$$

Eq. (43) is solved numerically on a computer by iteration. The load integrals are evaluated by Simpsons rule:

$$(46)\qquad \int_{\frac{1}{\gamma}}^{\eta} x\,dr = \frac{\Delta r}{3}\Bigg[\begin{Bmatrix} \left(\frac{5}{4}x_1 + 2x_2 - \frac{1}{4}x_3\right) + \left(x_2 + 4x_3 + 2x_4 + \text{----} + 4x_{\ell-1} + x_\ell\right) \\ \left(x_1 + 4x_2 + 2x_3 + \text{------------} + 4x_{\ell-1} + x_\ell\right) \end{Bmatrix}$$
$$+\left(\frac{\Delta r - \frac{3}{2}\delta}{\Delta r - \delta}\left(x_\ell + x_{\ell+4}\right) + \frac{(\Delta r)^2}{2\delta(\Delta r - \delta)}\left(x_{\ell+1} + x_{\ell+3}\right) + \frac{3\delta - \Delta r}{\delta}\,x_{\ell+2}\right)$$
$$+\begin{Bmatrix} \left(x_{\ell+4} + 4x_{\ell+5} + \text{----} + 4x_{m+1} + x_{m+2}\right) + \left(-\frac{1}{4}x_{m+1} + 2x_{m+2} + \frac{5}{4}x_{m+3}\right) \\ \left(x_{\ell+4} + 4x_{\ell+5} + 2x_{\ell+6} + \text{----------} + 4x_{m+2} + x_{m+3}\right) \end{Bmatrix}\Bigg]$$

$$(47)\qquad \int_0^{\frac{\pi}{N}} x\,d\theta = \frac{\Delta\theta}{3}\left[\frac{3\delta - \Delta\theta}{2\delta}x_1 + \frac{(\Delta\theta)^2}{2\delta(\Delta\theta - \delta)}x_2 + \frac{\Delta\theta - \frac{3}{2}\delta}{\Delta\theta - \delta}x_3 + \begin{Bmatrix} \left(x_3 + 4x_4 + \text{---} + x_{n+1}\right) + \left(-\frac{1}{4}x_n + 2x_{n+1} + \frac{5}{4}x_{n+2}\right) \\ \left(x_3 + 4x_4 + 2x_5 + \text{----} + 4x_{n+1} + x_{n+2}\right) \end{Bmatrix}\right]$$

Static Stiffness and Damping

As $\sigma \rightarrow 0$ it is seen from Eq. (31) that H becomes real and that Eq. (31) reduces to Eq. (20) so that H = u. Furthermore, for small values of σ G becomes proportional to σ as seen from Eq. (30). Hence, in the limit G becomes purely imaginary and is determined from the equation:

$$\frac{1}{r}\frac{\partial}{\partial r}\left[r\,\frac{\partial(\mathrm{Im}\{G\}/\sigma)}{\partial r}\right] + \frac{\partial^2(\mathrm{Im}\{G\}/\sigma)}{r^2\partial\theta^2} = -P_0 \tag{48}$$

Therefore, in calculating the stiffness only H contributes, i.e.

$$\frac{K_{static}}{\frac{1}{c}\pi(R_1^2-R_2^2)P_a} = \frac{\frac{3}{2}q}{1+\psi u_c}\cdot\frac{2N/\pi}{\eta^2-1/\gamma^2}\int_{\frac{1}{\gamma}}^{\eta}\int_0^{\frac{\pi}{N}}\frac{u}{\sqrt{1+qu}}\,r\,dr\,d\theta \tag{49}$$

When ψ is real the static damping becomes:

$$\frac{B}{\mu R_1\left(\frac{R_1}{c}\right)^2} = \frac{24N}{\eta^4}\left[\int_{\frac{1}{\gamma}}^{\eta}\int_0^{\frac{\pi}{N}}\frac{\mathrm{Im}\{G\}/\sigma}{P_0}\,r\,d\theta\,dr - \frac{\psi\,\mathrm{Im}\{G_c\}/\sigma}{1+\psi u_c}\int_{\frac{1}{\gamma}}^{\eta}\int_0^{\frac{\pi}{N}}\frac{u}{\sqrt{1+qu}}\,r\,d\theta\,dr\right] \tag{50}$$

Stability

Returning to Eq. (36), giving the dynamic load, it is shown through Eq. (37) and (38) that the real part represents the stiffness, the imaginary part the damping. Restricting the motion to be purely translatory, instability occurs when either the damping or the stiffness is negative. Thus the treshold of instability may be determined by setting either Eq. (37) or (38) equal to zero. For a particular calculation (i.e. given geometry, flow parameter q and frequency number σ) the only variable is ψ which, however, may be complex as explained previously. Since Eq. (37) and (38) afford two independent criteria each equation has actually two unknowns. It is convenient to solve each equation for the imaginary part of ψ as a function of the real part of ψ which is in general known, being given by Eq. (13). Both equations are quadratic.

CONCLUSIONS

1. Finite difference calculations can be used to solve the dynamic, source fed thrust bearing. The primary problem is to establish a method for selecting the effective area over which the gas enters the bearing.

2. The number of computer calculations can be minimized by a proper choice of variables and parameters.

3. The dynamic stiffness and damping as well as the static load can be computed for the source fed thrust bearing. The threshold of instability may be evaluated including the effect of feeder hole volume.

4. Indications are that the solution agrees with test results but only one numerical example has been obtained at present. The solution may be used to evaluate the previously established line source solution. One such comparison is given.

RECOMMENDATIONS

1. Compare the solution to experimental data to check the validity of the analysis and to evaluate the effective feeder hole area.

2. Upon completion of item 1, perform enough calculations to be able to make general design charts.

3. Extend the method to the externally pressurized journal bearing.

REFERENCES

1. MTI-62TR26: "Analysis of the Hydrostatic Journal and Thrust Gas Bearing for the NASA AB-5 Gyro Gimbal Bearing," by J.Lund, R.J. Wernick and S.B. Malanoski Prepared under Contract No. NAS 8-2588 for the National Aeronautical and Space Administration, Huntsville, Alabama. Oct. 23, 1962.

2. MTI-63TR29: "Spring and Damping Coefficients for the Tilting Pad Journal Bearing," by J. Lund.

APPENDIX

IBM 1620 Computer Program PN. 38: Static and Dynamic Stiffness of Source Fed Thrust Bearing

The input form is given on page 34. Below follow the instructions for preparing the input.

Card 1

Text Col. 2-52. This card is used for identification of the calculation.

Card 2

FORMAT 8·(1XI4)

Word 1 gives the number, m, of radial subdivisions used in the finite difference calculation, see Fig. 10. page 20 . Hence, the radial increment becomes $\Delta r = (R_1 - R_2)/m$. Around the feeding hole the program adds two additional subdivisions automatically to account for the actual feeding hole dimension. These two subdivisions should not be included in m. m must not exceed 25.

Word 2 gives the number, n, of circumferential subdivisions of the angle π/N for use in the finite difference calculation, see Fig. 10, page 20 . The circumferential increment thus becomes $\Delta\theta = (\pi/N)/n$. Around the feeding hole the program automatically adds a subdivision to account for the actual feeding hole dimension. This subdivision should not be included in the count for n. n must not exceed 13.

Word 3 gives the distance from the inner radius to the feeding hole as a number of radial subdivision Δr. Hence, the limits for the word are $1 \leq \text{word } 3 \leq (m-1)$. As before, word 3 does not include the sub-subdivisions added by the program automatically. Word 3 defines the radius of the feeding hole circle R_c:

(1A) $$R_c = R_2 + (\text{word } 3) \cdot \frac{R_1 - R_2}{m}$$

The program operates on dimensionless quantities such that all radial dimensions are made dimensionless with respect to R_c. With R_1/R_2 given as input the program uses internally:

(2A) $$\gamma = \frac{R_c}{R_2} = 1 + \frac{\frac{R_1}{R_2} - 1}{m} \quad \text{(Word 3)}$$

(3A) $$\eta = \frac{R_1}{R_c} = \frac{R_1/R_2}{\gamma}$$

Word 4 gives the total number N of feeding holes per 360°. Since there is symmetry around all radial lines through the feeding holes and all radial lines half way between feeding holes it is only necessary to calculate the pressure distribution for a radial sector between two such radial lines. Therefore, the sector extends over an angle π/N, see Fig. 10, page 20.

Word 5 NQ is the number of flow parameters q given in the input list below. NQ may not exceed 50. If NQ=0 the program only computes $u = (\gamma_0^2 - 1)/q$, see Eq. (20), page 16, and the q-list cannot be given. In that case the σ-list is not used and should therefore be excluded by setting NSIG=0.

Word 6 NSIG is the number of frequency numbers σ given in the input list below. NSIG may not exceed 25. If NSIG=0 no σ-list can be given. Hence, the program only calculates the static load based on the q-list. Note, that in this case only one pressure computation is performed by iteration, i.e. for calculating u.

Word 7 gives the maximum allowable number of iterations per calculation. If the calculation has not converged after the specified number of iterations the program prints out the results and proceeds as if convergence had been achieved.

Word 8 If word 8 is 0 the program returns to read in a new set of input data upon completion of the present input set. If word 8 is 1 the program stops upon completion of the present input set.

Card 3

FORMAT 5 • (1XE13.6)

Word 1 gives the ratio R_1/R_2 of the outer radius to the inner radius. Word 2 gives the ratio d/R_c of the feeding hole diameter to the radius of the feeding hole circle. Note that R_c is given indirectly through word 3, card 2. The program uses d/R_c to calculate the area over which the external flow enters the bearing. The program replaces this actual circular area by a square of the same areas with sides δ, i.e.

(4A) $$\delta = \frac{\sqrt{\pi}}{2}\left(\frac{d}{R_c}\right)$$

Then the program adds two radial sub-subdivisions, each of size δ, and one circumferential sub-subdivision, size δ, around the feeding hole as shown on Fig. 10, page 20. It is necessary that δ be less than both Δr and $\Delta\theta$, i.e.

(5A) $$\frac{d}{R_c} < \frac{2}{\sqrt{\pi}} \frac{\frac{R_1}{R_2} - 1}{m + \left(\frac{R_1}{R_2} - 1\right)(\text{word } 3, \text{card } 2)}$$

(6A) $$\frac{d}{R_c} < \frac{\pi/N}{n}$$

If this is not the case adjust m and n accordingly.

Word 3 gives the relative convergence limit δ_R for the finite difference calculation. Let the variable be denoted y_{ij} as in Eq. (43), page 20. After the kth iteration the program calculates:

(7A) $$\frac{\sum\sum |y_{ij}^{(k)} - y_{ij}^{(k-1)}|}{\sum\sum |y_{ij}^{(k)}|} - \delta_R = \Delta_R$$

Relative convergence is achieved when $\Delta_R \leq 0$. Note, that for y complex only the real part is used in forming Δ_R. A typical value is $\delta_R = .001$.

Word 4 gives the absolute convergence limit δ_A for the finite difference calculation. Let the variable be denoted y_{ij} as above. After the k'th iteration the program computes:

(8A) $$\Sigma_k = \sum_i \sum_j \left| Re\{y_{ij}^{(k)}\} \right|$$

Based on this value and the two preceding ones an exponentially extrapolated sum is determined:

(9A) $$\Sigma_k^x = \Sigma_k + \frac{(\Sigma_k - \Sigma_{k-1})^2}{(2\Sigma_{k-1} - \Sigma_k - \Sigma_{k-2})}$$

The program computes:

(10A) $$\frac{|\Sigma_k^x - \Sigma_k|}{\Sigma_k} - \delta_A = \Delta_A$$

Absolute convergence is achieved when $\Delta_A \leq 0$. The extrapolated sum cannot be calculated unless 3 consecutive values of Σ_k are available. Also Σ_k^x cannot be determined unless the Σ_k-sequence is monotonely increasing with decreasing slope. If these conditions are not satisfied the program sets arbitrarily $\Sigma_k^x = 10^{38}$ and $\Delta_A = 1$. For further details see Ref. 2. A typical value is δ_A = .001 to .005.

It should be noted that the number of iterations for convergence increases rapidly with decreasing δ_A. Hence, δ_A should be made as large as possible consistent with the desired accuracy. Also note that in general absolute convergence is more difficult to obtain than relative convergence.

Word 5 gives the limit δ_x for iteration extrpolation. After the k'th iteration the extrapolated sum Σ_k^x is calculated from Eq. (9A) above. When the sequence of Σ_k^x- values is monotonely increasing such that:

(11A) $$\frac{\Sigma_{k-1}^x - \Sigma_{k-2}^x}{\Sigma_{k-1}^x} - \delta_x \leq 0 \qquad \Sigma_{k-1}^x - \Sigma_{k-2}^x \geq 0$$

$$\frac{\Sigma_k^x - \Sigma_{k-1}^x}{\Sigma_k^x} - \delta_x \leq 0 \qquad \Sigma_k^x - \Sigma_{k-1}^x \geq 0$$

then the calculated $y_{ij}^{(k)}$ distribution is multiplied by Σ_k^x/Σ_k to speed up the convergence of the iterations. Hence, δ_x determines how "smooth" Σ_k^x must be before extrapolation is performed. A typical value is $\delta_x = 0.005$.

LIST OF FLOW PARAMETERS q

FORMAT 5·(1XE13.6)

(only if NQ ≠ 0)

Up to 10 cards with 5 q-values per card may be given. The total number of q-values is given by NQ, card 2. q is the dimensionless flow as given by Eq. (16) and determined as shown by Fig. 2. The actual total bearing mass flow M_0 is:

(12A) $$M_o = \frac{\pi P_a^2 C^3}{6\mu \mathcal{R} T} q \quad \frac{\text{lbs}}{\text{sec}}$$

(when $\mathcal{R}T$ is $\frac{\text{lbs-in}}{\text{lbs}}$)

LIST OF FREQUENCY NUMBERS σ

FORMAT 5·(1XE13.6)

(only if NSIG ≠ 0)

Up to 5 cards with 5 σ-values per card may be given. The total number of σ-values is given by NSIG, card 2. σ is the dimensionless frequency as given through Eq. (4), page 14 .

OUTPUT

The output first lists the input values. Next follows a list of the convergence of the u-calculation, given in 6 columns. The first column gives the iteration number. The column "REL.CON" gives the relative convergence error Δ_R, Eq. (7A). The column "ABS.CON" gives the absolute convergence error Δ_A, Eq. (10A). Note, that both Δ_R and Δ_A must be zero or negative for convergence. The column "SUM" is the summation of the variable over the complete field, Eq.(8A). The column "EXT.SUM" is the exponentially extrapolated sum, Eq.(9A). The last column "COUNT" gives the number of iterations after the last field extrapolation. Thereafter the u-distribution is listed, labeled "(PO**2-1)/Q DISTRIBUTION." The value of u at the orifice, u_c, is also given in the heading. In listing the u-distribution the following convention is used:

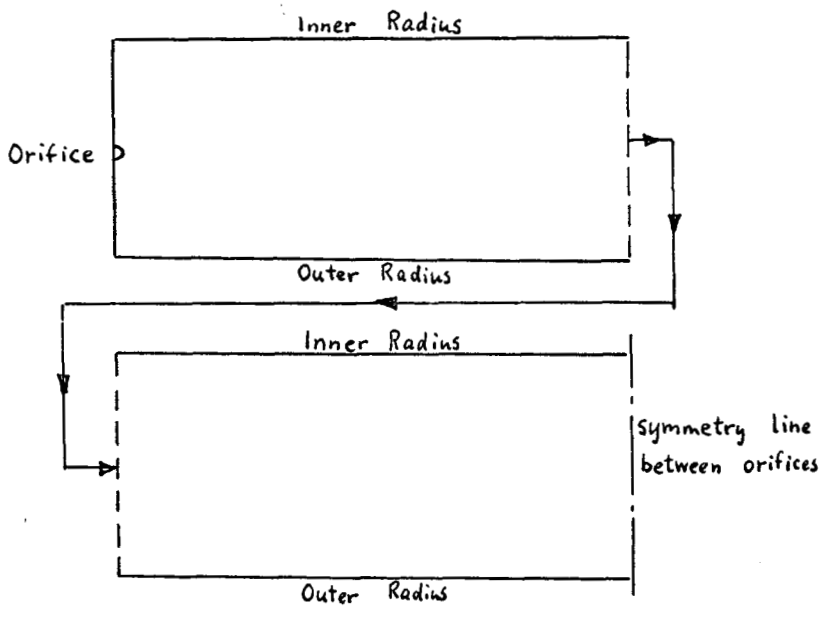

Next follows the first q-calculation. The static pressure distribution (P_o-1) is given and the dimensionless static load:

$$\text{"STATIC LOAD"} = \frac{W}{\pi(R_1^2-R_2^2)P_a}$$

After this the program calculates G and H for each frequency number σ. The G-calculation comes first with an iteration list followed by the G/P_o-distribution, both real and imaginary part given. Note, that the distribution is G/P_o, not G, whereas "RE(G)-ORIF" and "IM(G)-ORIF" gives G itself at the orifice, i.e. G_c. Each distribution is followed by the value of the integrated distribution with the labels:

"STIFFNESS" use in calculating $\dfrac{K}{\frac{1}{C}\pi(R_1^2-R_2^2)P_a}$ (Eq.(37))

"DAMPING 1" use in calculating $\dfrac{B}{\mu R_1 \left(\frac{R_1}{C}\right)^3}$ (Eq.(39))

"DAMPING 2" use in calculating $\dfrac{B\ \mathcal{R}TM_o}{P_a^2\ R_1^4}$ (Eq.(40))

The output for the H-calculation is completely analogous to the G-calculation. For each frequency number a G and an H calculation is given as described above. When all frequency numbers have been used the next q-calculation starts, giving first the static pressure and the static load. Then each frequency number is repeated as described above.

Program Operation

The program is written for the IBM 1620 computer with 60,000 bit storage. It is written in FORTRAN I and the program deck does not include subroutines. Input and output are on cards.

To give an idea about the computing time it took 90 minutes to run the calculation for the included numerical example. The field is 8·5 and 3 distributions are calculated, each with 70 iterations. Since the actual field is (8+1)·(5+2)=63, this means 1.2 seconds per point. Hence, for the same desired absolute convergence limit of .5 per cent the time may be estimated from:

$$\text{Computer time} = (1/4 + NQ \cdot NSIG) \cdot \left[(m+1)(n+2)\right]^2 \text{ seconds}$$

Note that the number of iterations for convergence increases roughly linearly with the mesh size, being about 70 iterations for 63 points. However, the magnitude of the feeding hole diameter also influences the number of iterations.

INPUT FOR IBM 1620 COMPUTER PROGRAM

PN0138: Static and Dynamic Stiffness of Source Fed Thrust Bearing

Card 1 Text, Col. 2-52

Card 2 FORMAT 8 · (1XI4)

_____ 1. m: Number of radial subdivisions ($m \leq 25$)

_____ 2. n: Number of circumferential subdivisions ($n \leq 13$)

_____ 3. Number of subdivisions from inner radius to feeding hole. $1 \leq$ item $\leq (m-1)$

_____ 4. N: Number of feeding holes per 360°

_____ 5. NQ: Number of flow parameter values, q, in input list ($NQ \leq 50$)

_____ 6. NSIG: Number of frequency number values, σ in input list ($NSIG \leq 25$)

_____ 7. Maximum allowable number of iterations

_____ 8. If 0: more input follows. If 1: last set of input

Card 3 FORMAT 5 · (1XE13.6)

_____ 1. R_1/R_2: Ratio of outer to inner radius

_____ 2. d/R_c: Ratio of feeding hole diameter to radius of orifice circle

_____ 3. δ_R: Relative convergence limit

_____ 4. δ_A: Absolute convergence limit

_____ 5. δ_x: Limit for extrapolation criterion

List of Flow Parameters: q FORMAT 5 · (1XE13.6) Only when $NQ \geq 1$

_____ _____ _____ _____ _____

_____ _____ _____ _____ _____

_____ _____ _____ _____ _____

List of Frequency Number: σ FORMAT 5 · (1XE13.6) only when $NSIG \geq 1$

_____ _____ _____ _____ _____

_____ _____ _____ _____ _____

_____ _____ _____ _____ _____

N0138-DYNAMIC STIFFN.OF SOURCE FED THRUST BRG.
TEST CASE 9-5-63 J.LUND RD 57

M	N	J-OR	N.OR	N.Q	N.SIG	CALC	INP
8	5	4	12	1	1	70	1

R1/R2	RC/R2	ORF.D	REL.LM	ABS.LM	EX.LM
1.50000E-00	1.25000E-00	3.00000E-02	1.00000E-03	5.00000E-03	5.00000E-03

FLOW PARAMETERS Q

1.500000E+01	.000000E-99	.000000E-99	.000000E-99	.000000E-99

FREQUENCY NUMBERS SIGMA

5.000000E-00	.000000E-99	.000000E-99	.000000E-99	.000000E-99

NO.IT	REL.CON	ABS.CON	SUM	EXT.SUM	COUNT
1	9.990000E-01	1.000000E-00	5.071565E-01	1.000000E+38	1
2	4.232983E-01	1.000000E-00	8.809366E-01	1.000000E+38	2
3	2.717830E-01	2.074943E-00	1.211379E-00	3.730980E-00	3
4	2.012163E-01	2.649480E-00	1.518431E-00	5.549078E-00	4
5	1.601496E-01	3.057427E-00	1.810133E-00	7.353535E-00	5
6	1.329211E-01	3.170977E-00	2.090033E-00	8.727930E-00	6
7	1.132563E-01	2.986991E-00	2.359637E-00	9.419650E-00	7
8	9.824009E-02	2.672869E-00	2.619607E-00	9.634573E-00	8
9	8.633762E-02	2.352914E-00	2.870291E-00	9.638192E-00	9
10	7.665102E-02	2.070922E-00	3.111936E-00	9.572075E-00	10
11	6.861068E-02	1.833797E-00	3.344768E-00	9.495118E-00	11
12	6.183258E-02	1.637126E-00	3.569019E-00	9.429798E-00	12
13	5.604599E-02	1.472725E-00	3.784934E-00	9.378027E-00	13
14	5.105326E-02	1.334150E-00	3.992771E-00	9.339693E-00	14
15	4.670618E-02	1.216137E-00	4.192794E-00	9.312771E-00	15
16	4.289121E-02	1.114260E-00	4.385268E-00	9.293526E-00	16
17	3.951977E-02	1.025734E-00	4.570463E-00	9.281395E-00	17
18	3.652178E-02	9.477484E-01	4.748640E-00	9.272900E-00	18
19	3.384101E-02	8.787961E-01	4.920060E-00	9.268391E-00	19
20	3.143180E-02	8.172777E-01	5.084975E-00	9.266238E-00	20
21	2.925684E-02	7.619278E-01	5.243631E-00	9.265118E-00	21
22	2.728521E-02	7.119795E-01	5.396266E-00	9.265278E-00	22
23	2.549113E-02	6.667534E-01	5.543109E-00	9.266712E-00	23
24	4.774176E-02	1.000000E-00	9.162204E-00	1.000000E+38	1
25	3.099480E-02	1.000000E-00	9.138338E-00	1.000000E+38	2
26	2.150869E-02	1.000000E-00	9.134973E-00	1.000000E+38	3
27	1.724356E-02	1.000000E-00	9.139043E-00	1.000000E+38	4
28	1.392227E-02	1.000000E-00	9.145464E-00	1.000000E+38	5
29	1.139447E-02	1.000000E-00	9.152158E-00	1.000000E+38	6
30	9.391084E-03	4.580431E-03	9.158408E-00	9.246149E-00	7
31	7.790817E-03	7.185742E-04	9.164050E-00	9.216455E-00	8
32	6.588068E-03	-8.542870E-05	9.169121E-00	9.214183E-00	9
33	5.589685E-03	-1.483465E-04	9.173717E-00	9.218225E-00	10
34	4.741555E-03	1.439772E-04	9.177937E-00	9.225148E-00	11
35	4.292204E-03	1.000000E-00	9.226486E-00	1.000000E+38	1
36	3.585118E-03	1.000000E-00	9.228283E-00	1.000000E+38	2
37	3.017803E-03	1.000000E-00	9.230124E-00	1.000000E+38	3
38	2.546458E-03	1.217489E-02	9.231945E-00	9.390502E-00	4
39	2.134529E-03	4.205631E-03	9.233728E-00	9.318730E-00	5
40	1.772339E-03	3.582246E-03	9.235472E-00	9.314733E-00	6
41	1.453060E-03	4.580452E-03	9.237184E-00	9.325680E-00	7
42	1.171109E-03	5.453663E-03	9.238866E-00	9.335446E-00	8
43	1.473984E-03	1.000000E-00	9.331818E-00	1.000000E+38	1
44	1.089312E-03	1.000000E-00	9.329561E-00	1.000000E+38	2
45	8.271055E-04	1.000000E-00	9.327734E-00	1.000000E+38	3

46	6.100662E-04	1.000000E-00	9.326127E-00	1.000000E+38	4	0
47	4.237267E-04	1.000000E-00	9.324657E-00	1.000000E+38	5	0
48	2.613000E-04	1.000000E-00	9.323285E-00	1.000000E+38	6	0
49	1.180980E-04	1.000000E-00	9.321993E-00	1.000000E+38	7	0
50	-8.525000E-06	1.000000E-00	9.320775E-00	1.000000E+38	8	0
51	-1.200136E-04	1.000000E-00	9.319624E-00	1.000000E+38	9	0
52	-2.189197E-04	1.000000E-00	9.318536E-00	1.000000E+38	10	0
53	-3.066279E-04	1.000000E-00	9.317509E-00	1.000000E+38	11	0
54	-3.841911E-04	1.000000E-00	9.316540E-00	1.000000E+38	12	0
55	-4.530547E-04	1.000000E-00	9.315624E-00	1.000000E+38	13	0
56	-5.141566E-04	1.000000E-00	9.314759E-00	1.000000E+38	14	0
57	-5.683684E-04	1.000000E-00	9.313942E-00	1.000000E+38	15	0
58	-6.164525E-04	1.000000E-00	9.313168E-00	1.000000E+38	16	0
59	-6.591207E-04	1.000000E-00	9.312437E-00	1.000000E+38	17	0
60	-6.969703E-04	1.000000E-00	9.311745E-00	1.000000E+38	18	0
61	-7.305388E-04	1.000000E-00	9.311089E-00	1.000000E+38	19	0
62	-7.603008E-04	1.000000E-00	9.310467E-00	1.000000E+38	20	0
63	-7.867198E-04	1.000000E-00	9.309877E-00	1.000000E+38	21	0
64	-8.101435E-04	1.000000E-00	9.309316E-00	1.000000E+38	22	0
65	-8.309262E-04	1.000000E-00	9.308784E-00	1.000000E+38	23	0
66	-8.493713E-04	1.000000E-00	9.308277E-00	1.000000E+38	24	0
67	-8.657332E-04	1.000000E-00	9.307795E-00	1.000000E+38	25	0
68	-8.802671E-04	1.000000E-00	9.307336E-00	1.000000E+38	26	0
69	-8.931475E-04	1.000000E-00	9.306899E-00	1.000000E+38	27	0
70	-9.045835E-04	1.000000E-00	9.306482E-00	1.000000E+38	28	0

(P0**2-1)/Q DISTRIBUTION-AT ORIFICE= 6.525240E-01

.000000E-99	.000000E-99	.000000E-99	.000000E-99	.000000E-99
7.456124E-02	7.316842E-02	6.961326E-02	5.821525E-02	4.756088E-02
1.579774E-01	1.530746E-01	1.420877E-01	1.121882E-01	8.792041E-02
2.783273E-01	2.563019E-01	2.217384E-01	1.570707E-01	1.156582E-01
3.910366E-01	3.211487E-01	2.550309E-01	1.692996E-01	1.216298E-01
6.525240E-01	3.911891E-01	2.754113E-01	1.732197E-01	1.224099E-01
3.894085E-01	3.171203E-01	2.498674E-01	1.639563E-01	1.167028E-01
2.755242E-01	2.511226E-01	2.142767E-01	1.482457E-01	1.071762E-01
1.527520E-01	1.467192E-01	1.338333E-01	1.010337E-01	7.611471E-02
6.982010E-02	6.798191E-02	6.349341E-02	5.011196E-02	3.874211E-02
.000000E-99	.000000E-99	.000000E-99	.000000E-99	.000000E-99

.000000E-99	.000000E-99
4.057123E-02	3.818342E-02
7.319864E-02	6.834085E-02
9.328466E-02	8.624283E-02
9.709202E-02	8.949130E-02
9.705032E-02	8.926688E-02
9.255538E-02	8.510290E-02
8.536220E-02	7.855131E-02
6.164081E-02	5.696618E-02
3.176091E-02	2.945432E-02
.000000E-99	.000000E-99

FLOW PARAMETER Q= 1.500000E+01

STATIC PRESSURE (PO-1) DISTRIB.,PO AT ORIFICE= 3.284487E-00

.000000E-99	.000000E-99	.000000E-99	.000000E-99	.000000E-99
4.554788E-01	4.482839E-01	4.297548E-01	3.686594E-01	3.089741E-01
8.356639E-01	8.155217E-01	7.695525E-01	6.379327E-01	5.227626E-01
1.274842E-00	1.201029E-00	1.079922E-00	8.319556E-01	6.537455E-01
1.620219E-00	1.411893E-00	1.196693E-00	8.813542E-01	6.806093E-01
2.284487E-00	1.620655E-00	1.265208E-00	8.969173E-01	6.840871E-01
1.615554E-00	1.399334E-00	1.178993E-00	8.599315E-01	6.584760E-01
1.265582E-00	1.183309E-00	1.052839E-00	7.954628E-01	6.148202E-01
8.141886E-01	7.890747E-01	7.342145E-01	5.860348E-01	4.634618E-01
4.308394E-01	4.211715E-01	3.972834E-01	3.235102E-01	2.574305E-01
.000000E-99	.000000E-99	.000000E-99	.000000E-99	.000000E-99

.000000E-99	.000000E-99
2.682935E-01	2.540938E-01
4.484404E-01	4.230645E-01
5.489576E-01	5.144776E-01
5.672843E-01	5.304801E-01
5.670848E-01	5.293800E-01
5.454225E-01	5.088218E-01
5.101102E-01	4.758962E-01
3.873039E-01	3.617975E-01
2.150776E-01	2.007559E-01
.000000E-99	.000000E-99

STATIC LOAD= 5.412825E-01

FREQUENCY NUMBER= 5.000000E-00

NO.IT	REL.CON	ABS.CON	SUM	EXT.SUM	COUNT
1	9.990000E-01	1.000000E-00	8.490975E-04	1.000000E+38	1
2	6.345953E-01	1.000000E-00	2.330093E-03	1.000000E+38	2
3	4.600740E-01	1.000000E-00	4.323588E-03	1.000000E+38	3
4	3.585609E-01	1.000000E-00	6.750977E-03	1.000000E+38	4
5	2.925967E-01	1.000000E-00	9.556835E-03	1.000000E+38	5
6	2.463341E-01	1.000000E-00	1.269731E-02	1.000000E+38	6
7	2.120965E-01	1.000000E-00	1.613578E-02	1.000000E+38	7
8	1.856661E-01	1.000000E-00	1.983907E-02	1.000000E+38	8
9	1.645568E-01	1.000000E-00	2.377522E-02	1.000000E+38	9
10	1.472324E-01	1.000000E-00	2.791280E-02	1.000000E+38	10
11	1.326996E-01	1.000000E-00	3.222070E-02	1.000000E+38	11
12	1.202912E-01	1.000000E-00	3.666824E-02	1.000000E+38	12
13	1.095441E-01	1.000000E-00	4.122547E-02	1.000000E+38	13
14	1.001272E-01	1.000000E-00	4.586353E-02	1.000000E+38	14
15	9.179709E-02	1.000000E-00	5.055487E-02	1.000000E+38	15
16	8.437007E-02	1.000000E-00	5.527359E-02	1.000000E+38	16
17	7.770478E-02	1.000000E-00	5.999552E-02	1.000000E+38	17
18	7.169040E-02	1.801134E+01	6.469848E-02	1.230328E-00	18
19	6.623833E-02	8.004888E-00	6.936229E-02	6.249465E-01	19
20	6.127696E-02	5.005247E-00	7.396884E-02	4.445710E-01	20
21	5.674736E-02	3.568527E-00	7.850214E-02	3.590317E-01	21
22	5.260057E-02	2.727149E-00	8.294821E-02	3.095750E-01	22
23	4.879536E-02	2.177581E-00	8.729510E-02	2.778238E-01	23
24	4.529663E-02	1.790979E-00	9.153276E-02	2.559236E-01	24
25	4.207419E-02	1.505520E-00	9.565292E-02	2.401386E-01	25
26	3.910185E-02	1.286865E-00	9.964904E-02	2.283822E-01	26
27	3.635669E-02	1.113887E-00	1.035160E-01	2.193388E-01	27
28	3.381853E-02	9.745937E-01	1.072503E-01	2.123120E-01	28
29	3.146943E-02	8.602099E-01	1.108495E-01	2.067576E-01	29
30	2.929339E-02	7.646495E-01	1.143124E-01	2.022929E-01	30
31	2.727601E-02	6.836957E-01	1.176387E-01	1.986561E-01	31
32	2.540443E-02	6.148334E-01	1.208292E-01	1.957232E-01	32
33	2.366691E-02	5.550986E-01	1.238850E-01	1.932729E-01	33
34	2.205282E-02	5.034158E-01	1.268083E-01	1.912797E-01	34
35	2.055255E-02	4.578346E-01	1.296016E-01	1.895857E-01	35
36	1.915727E-02	4.179731E-01	1.322677E-01	1.882134E-01	36
37	1.785898E-02	3.823224E-01	1.348101E-01	1.870251E-01	37
38	1.665025E-02	3.507063E-01	1.372323E-01	1.860467E-01	38
39	1.552441E-02	3.221812E-01	1.395380E-01	1.851923E-01	39
40	1.447525E-02	2.970696E-01	1.417314E-01	1.845442E-01	40
41	1.349714E-02	2.735608E-01	1.438163E-01	1.838779E-01	41
42	1.258482E-02	2.532307E-01	1.457969E-01	1.834462E-01	42
43	1.173347E-02	2.339741E-01	1.476774E-01	1.829685E-01	43
44	1.093874E-02	2.166746E-01	1.494618E-01	1.825937E-01	44
45	1.019652E-02	2.009598E-01	1.511542E-01	1.822858E-01	45
46	9.503070E-03	1.866962E-01	1.527586E-01	1.820419E-01	46
47	8.854950E-03	1.731987E-01	1.542790E-01	1.817713E-01	47
48	8.248929E-03	1.611949E-01	1.557192E-01	1.815990E-01	48
49	7.682107E-03	1.499201E-01	1.570830E-01	1.814184E-01	49
50	7.151741E-03	1.397331E-01	1.583741E-01	1.812961E-01	50
51	6.655299E-03	1.298596E-01	1.595958E-01	1.811189E-01	51
52	6.190495E-03	1.211731E-01	1.607517E-01	1.810343E-01	52
53	5.755159E-03	1.130544E-01	1.618450E-01	1.809515E-01	53
54	5.347281E-03	1.053820E-01	1.628788E-01	1.808577E-01	54
55	4.965024E-03	9.828031E-02	1.638562E-01	1.807794E-01	55
56	4.606692E-03	9.176522E-02	1.647801E-01	1.807251E-01	56
57	4.270672E-03	8.560034E-02	1.656532E-01	1.806614E-01	57
58	3.955485E-03	8.001291E-02	1.664782E-01	1.806310E-01	58

59	3.659804E-03	7.462555E-02	1.672576E-01	1.805755E-01	59	1
60	3.382319E-03	6.975500E-02	1.679938E-01	1.805522E-01	60	1
61	3.121877E-03	6.509347E-02	1.686891E-01	1.805131E-01	61	1
62	2.877352E-03	6.071348E-02	1.693457E-01	1.804740E-01	62	1
63	2.647751E-03	5.679121E-02	1.699657E-01	1.804681E-01	63	1
64	2.432094E-03	5.297735E-02	1.705510E-01	1.804391E-01	64	1
65	2.229486E-03	4.947370E-02	1.711036E-01	1.804243E-01	65	1
66	2.039155E-03	4.616962E-02	1.716252E-01	1.804072E-01	66	1
67	1.860266E-03	4.307643E-02	1.721175E-01	1.803923E-01	67	2
68	1.692132E-03	4.011804E-02	1.725821E-01	1.803687E-01	68	2
69	1.534082E-03	3.750464E-02	1.730206E-01	1.803747E-01	69	2
70	1.385488E-03	3.496168E-02	1.734343E-01	1.803650E-01	70	2

RE(G)/PO Q= 1.500000E+01 SIG= 5.000000E-00 RE(G)-ORIF= 2.909649E-03 2

.000000E-99	.000000E-99	.000000E-99	.000000E-99	.000000E-99	2
1.034136E-03	1.047343E-03	1.080900E-03	1.187237E-03	1.296653E-03	2
1.343239E-03	1.371742E-03	1.443363E-03	1.661792E-03	1.882475E-03	2
1.254816E-03	1.313594E-03	1.435625E-03	1.761824E-03	2.073533E-03	2
1.107781E-03	1.220966E-03	1.388313E-03	1.760129E-03	2.099017E-03	2
8.858760E-04	1.128341E-03	1.354377E-03	1.760258E-03	2.114838E-03	2
1.100594E-03	1.217322E-03	1.388272E-03	1.766820E-03	2.111800E-03	2
1.238934E-03	1.302212E-03	1.430471E-03	1.769323E-03	2.091861E-03	2
1.299290E-03	1.330723E-03	1.408317E-03	1.644775E-03	1.881163E-03	2
9.653320E-04	9.795819E-04	1.016045E-03	1.132514E-03	1.248908E-03	2
.000000E-99	.000000E-99	.000000E-99	.000000E-99	.000000E-99	2

.000000E-99	.000000E-99	
1.377521E-03	1.407964E-03	
2.046645E-03	2.108572E-03	
2.300594E-03	2.385508E-03	
2.342453E-03	2.433090E-03	
2.366816E-03	2.460292E-03	
2.359139E-03	2.450963E-03	
2.325575E-03	2.412437E-03	
2.054317E-03	2.118658E-03	
1.332231E-03	1.362752E-03	
.000000E-99	.000000E-99	

STIFFNESS	DAMPING 1	DAMPING 2
1.472077E-03	4.282100E-03	2.802628E-03

IM(G)/PO Q= 1.500000E+01 SIG= 5.000000E-00 IM(G)-ORIF= 1.122277E-01

.000000E-99	.000000E-99	.000000E-99	.000000E-99	.000000E-99
3.693059E-02	3.711932E-02	3.762037E-02	3.905098E-02	4.024052E-02
4.829053E-02	4.885085E-02	5.025573E-02	5.401350E-02	5.714749E-02
4.684651E-02	4.838525E-02	5.129061E-02	5.771436E-02	6.266200E-02
4.212054E-02	4.563731E-02	5.008764E-02	5.779923E-02	6.332138E-02
3.416902E-02	4.257268E-02	4.910943E-02	5.779705E-02	6.361101E-02
4.193516E-02	4.556231E-02	5.008103E-02	5.779938E-02	6.328062E-02
4.641944E-02	4.808574E-02	5.110863E-02	5.757423E-02	6.245731E-02
4.718659E-02	4.780590E-02	4.927679E-02	5.306706E-02	5.609603E-02
3.506029E-02	3.525716E-02	3.575747E-02	3.710638E-02	3.810100E-02
.000000E-99	.000000E-99	.000000E-99	.000000E-99	.000000E-99

.000000E-99	.000000E-99
4.099086E-02	4.124562E-02
5.920062E-02	5.991666E-02
6.578995E-02	6.686726E-02
6.672570E-02	6.788950E-02

6.712201E-02	6.831491E-02
6.663575E-02	6.777770E-02
6.549660E-02	6.653366E-02
5.800120E-02	5.864892E-02
3.865750E-02	3.883211E-02
.000000E-99	.000000E-99

STIFFNESS	DAMPING 1	DAMPING 2
4.307226E-02	1.340137E-01	8.771508E-02

NO. IT	REL.CON	ABS.CON	SUM	EXT.SUM	COUNT
1	9.990000E-01	1.000000E-00	5.071563E-01	1.000000E+38	1
2	4.232980E-01	1.000000E-00	8.809358E-01	1.000000E+38	2
3	2.717822E-01	2.074885E-00	1.211377E-00	3.730903E-00	3
4	2.012151E-01	2.649229E-00	1.518425E-00	5.548676E-00	4
5	1.601477E-01	3.057088E-00	1.810123E-00	7.352881E-00	5
6	1.329186E-01	3.170082E-00	2.090015E-00	8.725987E-00	6
7	1.132533E-01	2.985675E-00	2.359608E-00	9.416430E-00	7
8	9.823635E-02	2.671995E-00	2.619564E-00	9.632128E-00	8
9	8.633317E-02	2.351564E-00	2.870231E-00	9.634117E-00	9
10	7.664583E-02	2.069390E-00	3.111854E-00	9.567054E-00	10
11	6.860476E-02	1.832486E-00	3.344657E-00	9.490422E-00	11
12	6.182592E-02	1.635638E-00	3.568875E-00	9.424109E-00	12
13	5.603858E-02	1.471371E-00	3.784753E-00	9.372453E-00	13
14	5.104506E-02	1.332646E-00	3.992545E-00	9.333161E-00	14
15	4.669723E-02	1.214483E-00	4.192517E-00	9.305223E-00	15
16	4.288147E-02	1.112758E-00	4.384934E-00	9.286233E-00	16
17	3.950922E-02	1.024162E-00	4.570064E-00	9.273403E-00	17
18	3.651046E-02	9.461033E-01	4.748170E-00	9.264171E-00	18
19	3.382886E-02	8.771022E-01	4.919511E-00	9.259024E-00	19
20	3.141885E-02	8.155321E-01	5.084340E-00	9.256204E-00	20
21	2.924309E-02	7.602334E-01	5.242902E-00	9.254946E-00	21
22	2.727060E-02	7.101690E-01	5.395434E-00	9.254082E-00	22
23	2.547572E-02	6.648976E-01	5.542167E-00	9.254852E-00	23
24	2.383672E-02	6.235223E-01	5.683322E-00	9.255417E-00	24
25	4.474987E-02	1.000000E-00	9.157723E-00	1.000000E+38	1
26	2.908657E-02	1.000000E-00	9.135450E-00	1.000000E+38	2
27	2.023310E-02	1.000000E-00	9.132334E-00	1.000000E+38	3
28	1.622141E-02	1.000000E-00	9.136148E-00	1.000000E+38	4
29	1.310173E-02	1.000000E-00	9.142138E-00	1.000000E+38	5
30	1.071987E-02	1.000000E-00	9.148360E-00	1.000000E+38	6
31	8.830611E-03	3.342943E-03	9.154143E-00	9.230516E-00	7
32	7.323670E-03	-1.361290E-05	9.159336E-00	9.205008E-00	8
33	6.192304E-03	-7.635637E-04	9.163975E-00	9.202798E-00	9
34	5.247263E-03	-9.027506E-04	9.168150E-00	9.205714E-00	10
35	4.444092E-03	-7.531952E-04	9.171954E-00	9.210905E-00	11
36	3.985213E-03	1.000000E-00	9.212275E-00	1.000000E+38	1
37	3.325300E-03	1.000000E-00	9.213981E-00	1.000000E+38	2
38	2.793991E-03	1.000000E-00	9.215688E-00	1.000000E+38	3
39	2.350447E-03	1.063208E-03	9.217347E-00	9.273233E-00	4
40	1.961673E-03	-2.462466E-04	9.218946E-00	9.262771E-00	5
41	1.619641E-03	-3.754197E-04	9.220490E-00	9.263131E-00	6
42	1.318001E-03	-1.805384E-04	9.221984E-00	9.266429E-00	7
43	1.307567E-03	1.000000E-00	9.265436E-00	1.000000E+38	1
44	9.939654E-04	1.000000E-00	9.265047E-00	1.000000E+38	2
45	7.524613E-04	1.000000E-00	9.264827E-00	1.000000E+38	3
46	5.455247E-04	1.000000E-00	9.264685E-00	1.000000E+38	4
47	3.651990E-04	1.000000E-00	9.264581E-00	1.000000E+38	5
48	2.071267E-04	1.000000E-00	9.264497E-00	1.000000E+38	6
49	6.786230E-05	1.000000E-00	9.264428E-00	1.000000E+38	7
50	-5.509750E-05	1.000000E-00	9.264369E-00	1.000000E+38	8

51	-1.637919E-04	1.000000E-00	9.264319E-00	1.000000E+38	9	3
52	-2.598887E-04	1.000000E-00	9.264275E-00	1.000000E+38	10	3
53	-3.448829E-04	1.000000E-00	9.264236E-00	1.000000E+38	11	3
54	-4.200898E-04	1.000000E-00	9.264201E-00	1.000000E+38	12	3
55	-4.865849E-04	1.000000E-00	9.264170E-00	1.000000E+38	13	3
56	-5.454537E-04	1.000000E-00	9.264139E-00	1.000000E+38	14	3
57	-5.975034E-04	1.000000E-00	9.264109E-00	1.000000E+38	15	3
58	-6.435662E-04	1.000000E-00	9.264079E-00	1.000000E+38	16	3
59	-6.843202E-04	1.000000E-00	9.264047E-00	1.000000E+38	17	3
60	-7.203373E-04	1.000000E-00	9.264014E-00	1.000000E+38	18	3
61	-7.521849E-04	1.000000E-00	9.263977E-00	1.000000E+38	19	3
62	-7.803784E-04	1.000000E-00	9.263937E-00	1.000000E+38	20	3
63	-8.052941E-04	1.000000E-00	9.263894E-00	1.000000E+38	21	3
64	-8.272951E-04	1.000000E-00	9.263847E-00	1.000000E+38	22	3
65	-8.467726E-04	1.000000E-00	9.263796E-00	1.000000E+38	23	3
66	-8.639700E-04	1.000000E-00	9.263740E-00	1.000000E+38	24	3
67	-8.791951E-04	1.000000E-00	9.263679E-00	1.000000E+38	25	3
68	-8.926163E-04	1.000000E-00	9.263615E-00	1.000000E+38	26	3
69	-9.044841E-04	1.000000E-00	9.263546E-00	1.000000E+38	27	3
70	-9.149730E-04	1.000000E-00	9.263472E-00	1.000000E+38	28	3

RE(H)/P0 Q= 1.500000E+01 SIG= 5.000000E-00 RE(H)-ORIF= 6.514136E-01

.000000E-99	.000000E-99	.000000E-99	.000000E-99	.000000E-99
5.095958E-02	5.025467E-02	4.842697E-02	4.228026E-02	3.608616E-02
8.566153E-02	8.391755E-02	7.990259E-02	6.810483E-02	5.735049E-02
1.219091E-01	1.159996E-01	1.061574E-01	8.528070E-02	6.947402E-02
1.488247E-01	1.327141E-01	1.156416E-01	8.951656E-02	7.189389E-02
1.983303E-01	1.488613E-01	1.211359E-01	9.084578E-02	7.220690E-02
1.484835E-01	1.317469E-01	1.142295E-01	8.769446E-02	6.990315E-02
1.212019E-01	1.146013E-01	1.039565E-01	8.213438E-02	6.593318E-02
8.384736E-02	8.165778E-02	7.682327E-02	6.335470E-02	5.166367E-02
4.857281E-02	4.761275E-02	4.522102E-02	3.764923E-02	3.060207E-02
.000000E-99	.000000E-99	.000000E-99	.000000E-99	.000000E-99

.000000E-99	.000000E-99
3.174469E-02	3.020495E-02
5.015078E-02	4.763980E-02
5.975937E-02	5.648151E-02
6.146817E-02	5.799217E-02
6.144822E-02	5.788614E-02
5.942323E-02	5.593720E-02
5.608825E-02	5.278446E-02
4.408703E-02	4.148780E-02
2.593449E-02	2.432715E-02
.000000E-99	.000000E-99

STIFFNESS	DAMPING 1	DAMPING 2
5.708072E-02	1.660410E-01	1.086736E-01

IM(H)/P0 Q= 1.500000E+01 SIG= 5.000000E-00 IM(H)-ORIF=-7.388997E-03

.000000E-99	.000000E-99	.000000E-99	.000000E-99	.000000E-99
-2.000874E-03	-2.008901E-03	-2.020150E-03	-2.027071E-03	-2.010638E-03
-2.861683E-03	-2.887784E-03	-2.934478E-03	-3.025270E-03	-3.070474E-03
-2.990993E-03	-3.077514E-03	-3.209673E-03	-3.437702E-03	-3.563091E-03
-2.751355E-03	-2.967775E-03	-3.200347E-03	-3.506376E-03	-3.660089E-03
-2.249665E-03	-2.788550E-03	-3.157568E-03	-3.522292E-03	-3.688124E-03
-2.733218E-03	-2.955268E-03	-3.189712E-03	-3.488812E-03	-3.630969E-03
-2.955113E-03	-3.047508E-03	-3.183134E-03	-3.401327E-03	-3.507218E-03
-2.777710E-03	-2.803726E-03	-2.847692E-03	-2.919133E-03	-2.932959E-03
-1.391829E-03	-1.896500E-03	-1.900108E-03	-1.881203E-03	-1.832954E-03

```
   .000000E-99   .000000E-99   .000000E-99   .000000E-99   .000000E-99
   .000000E-99   .000000E-99                                                3
 -1.989184E-03 -1.982646E-03                                                3
 -3.084274E-03 -3.090658E-03                                                3
 -3.416701E-03 -3.436014E-03                                                3
 -3.723843E-03 -3.745866E-03                                                3
 -3.753204E-03 -3.774899E-03                                                3
 -3.684351E-03 -3.701877E-03                                                3
 -3.542750E-03 -3.554128E-03                                                3
 -2.918234E-03 -2.912304E-03                                                3
 -1.785776E-03 -1.768667E-03                                                3
   .000000E-99   .000000E-99                                                3

   STIFFNESS     DAMPING 1     DAMPING 2                                    3
 -2.546209E-03 -7.406623E-03 -4.847624E-03                                  3
```

NOMENCLATURE

a	=	Orifice radius, inch
A_D, B_D, C_D, D_D	=	Dynamic load components, see Eqs. (33) and (34)
B	=	Damping coefficients, lbs-sec/in.
C	=	Clearance, inch
d	=	Feeder hole diameter, inch
E_D, F_D	=	Dynamic orifice parameters, see Eq. (35)
G, H	=	Dynamic pressure components, see Eq.(27)
G_c, H_c	=	Values of G and H at orifice
h	=	Film thickness divided by clearance
i, j	=	Finite difference coordinates, Fig. 10
K	=	Stiffness, lbs/in.
k	=	Ratio of specific heats
ℓ	=	Number of subdivisions from inner radius to orifice
M, M_o	=	Mass flow through one orifice, lbs-sec/in.
M_T	=	Total bearing mass flow, lbs-sec/in.
m	=	Dimensionless orifice mass flow, see Eqs.(7) and (22)
m_o	=	Dimensionless orifice mass flow under static conditions
m	=	Number of radial subdivisions
n	=	Number of circumferential subdivisions
N	=	Number of feeder holes per 360°
P_a	=	Ambient pressure, psia
P_s	=	Supply pressure, psia
P	=	Film pressure divided by P_a
P_o	=	Dimensionless film pressure under static conditions

P_{oc}	=	Dimensionless downstream orifice pressure, static conditions
P_1	=	Dimensionless dynamic pressure
q	=	$= \Lambda_t V m_o$, flow parameter
R_1	=	Outer radius of thrust bearing, inch.
R_2	=	Inner radius of thrust bearing, inch
R_c	=	Radius of feeder hole circle, inch
r	=	Radial coordinate divided by R_c
$\mathcal{R} \cdot T$	=	(Gas constant) · (Total temperature), in^2/sec^2.
t	=	Time, sec.
u	=	$= (P_o^2-1)/q$, dimensionless static pressure
u_c	=	Value of u at orifice
V	=	$= P_s/P_a$, pressure ratio
V_c	=	Volume of feeder hole, in^3
W	=	Load, lbs.
W_D	=	Dynamic load, lbs.
γ	=	$= R_c/R_2$
$\Delta r, \Delta\theta$	=	Radial and circumferential subdivision
Δ_A	=	Error in absolute covergence
Δ_R	=	Error in relative convergence
δ	=	Subdivision around feeder hole
δ_A	=	Absolute convergence limit
δ_R	=	Relative convergence limit
δ_x	=	Limit for extrapolation
ϵ	=	Vibration amplitude divided by clearance
η	=	$= R_1/R_c$
θ	=	Angular coordinate, rad.

μ	=	Viscosity, lbs-sec/in^2
ν	=	Orifice vena contracta coefficient
ρ	=	Density, lbs-sec^2/in^4
σ	=	$=(12\mu\omega/P_a) \cdot (\frac{R_c}{C})^2$, frequency number
τ	=	$=\omega t$, dimensionless time
ψ	=	$= - (\Lambda_t/2P_{oc}) \cdot \partial m/\partial(\frac{P_c}{V})$, orifice flow coefficient
ω	=	Frequency, rad/sec.